UCRL 15076

MASTER

INSTRUMENT SELECTION, INSTALLATION, AND ANALYSIS OF DATA FOR THE SPENT FUEL MINE-BY, NEVADA TEST SITE, CLIMAX STOCK

P.O. 4151809

By

T. Schrauf
M. Board

TR79-51
Terra Tek, Inc.
July, 1979

TerraTek

UNIVERSITY RESEARCH PARK · 420 WAKARA WAY · SALT LAKE CITY, UTAH 84108 · (801) 582-2220

INSTRUMENT SELECTION, INSTALLATION,
AND ANALYSIS OF DATA FOR THE
SPENT FUEL MINE-BY, NEVADA TEST SITE, CLIMAX STOCK

By

T. Schrauf
M. Board

TR79-51
Terra Tek, Inc.
July, 1979

TABLE OF CONTENTS

LIST OF FIGURES

LIST OF FIGURES (continued)

LIST OF FIGURES (Continued)

LIST OF TABLES

ABSTRACT

During the time period of February to April, 1979, Terra Tek personnel installed, calibrated and monitored twelve rod extensometers and twenty-two convergence measurement points in support of the spent fuel mine-by experiment at the Climax Stock in granite. This report details the instrumentation, installation, calibration, monitoring and subsequent analysis of the data.

Extensometer performance was good to excellent. Readings taken during heading and bench advance shows good instrument stability, with little or no anchor creep or slippage. Repeat calibrations indicate excellent repeatability. Convergence measurements proved to be somewhat disappointing. Measurement points within the heater drifts indicate little closure. Convergence pins within the spent fuel drift were subjected to significant blast damage that resulted in a discontinuous record.

A numerical analysis of the stresses and displacements of the rock mass as a result of the mine-by was performed. Two methods, finite element and displacement discontinuity, were used to model the mine-by. The results show an excellent agreement of the two methods. A comparison of the actual to predicted displacements show a good agreement for the 33^0 and 50^0 extensometers for a rock mass modulus of $3\text{-}5\times10^6$ psi and Poisson's ratio of .2. The horizontal extensometers however indicate a convergence of anchor and collar, whereas the prediction indicates a divergence. In addition, the IRAD stressmeters installed within the pillar indicate a significant reduction in vertical compression during mining of

the heading. These phenomena indicate that the pillar has been unloaded and a stress arch formed around the openings. The modulus of the pillar was reduced and the finite element code re-run to try to account for the unloading of the pillar. It is shown that a simple reduction of pillar modulus will not account for the observed stress and displacement changes. Varying the ratio of vertical to horizontal stress ratio over the range .8 to 1.25 also did not account for observed stresses and displacements. Based on this analysis, it is concluded that the displacements and stresses are a result of block motion or joint slippage within the pillars. This is primarily the result of the small dimensions of the pillars in relation to the spent fuel and heater drifts. This joint slippage can account for the formation of a stable stress arch around the openings and thus a relaxation of the pillar.

INTRODUCTION

Twelve extensometers and 22 convergence measurement points were installed at the Nevada Test Site, Area 15 shaft, to monitor rock mass movements associated with mining of the spent fuel canister drift. The purpose of this program was to determine and evaluate rock mass movements and to compare these measured displacements with those predicted from finite element models. The first section of this report deals with the selection, installation, calibration, and performance of the instrumentation. A second section covers the finite element and displacement continuity modeling and its comparison with the actual field data.

INSTRUMENTATION

Instrument Selection

The instruments selected for this project were multipoint rod extensometers (Terrametrics model CSLT-R) and a convergence point measuring tape (Terrametric model TE-75).

The rod extensometers measure displacement between 3 or 5 downhole anchors and the borehole collar. Instrument lengths ranged between 17 and 45 feet. These instruments featured hydraulic bladder anchors with 1/4 inch mild steel connecting rods for transmitting anchor displacements to the borehole collar. A 1 1/4 inch (32 mm) waterproofed flexible conduit was used to protect the connecting rods from corrosion. The connecting rods were spring tensioned to approximately 100 lbs. (450 N) and fitted with teflon spacers about every 15 feet (4.6 m) to reduce rod friction due to sagging and twisting of the rods downhole. Differential movements between the rod ends and the borehole collars were measured by means of linear potentiometers with a total displacement range of 25 mm and a response of about 0.4 volts/mm. Overall extensometer precision is about 0.02 mm.

The convergence point measuring tape consists of a standard steel surveyor's tape used in conjunction with a dial indicator. The instrument provides a constant spring tension for all readings to obtain maximum repeatability. Although readings are taken to the nearest 0.01 mm, actual precision is approximately 0.1 mm.

Instrument Locations

The rod extensometers are located in two measurement planes perpendicular to the spent fuel canister drift. These two measurement planes intersect the canister drift at its survey coordinates 2+83' amd 3+45'. A total of six extensometers are located in each measurement plane, three extending from the south heater drift and three extending from the north heater drift, as shown in Figure 1. Exact anchor depths are listed in Table 1.

The location of the convergence anchor points is shown in Figure 2.

Field Installation

Extensometer construction and installation can be subdivided into three separate tasks: (1) construction of downhole portion, (2) installation into borehole, and (3) installation of head assembly.

Construction of the downhole portion involved assembly of rods, anchors and pressurizing lines, and conduit section. This job was handled on a long workbench to accommodate the entire instrument during assembly. A two-man crew was required for the job. Procedure was as follows:

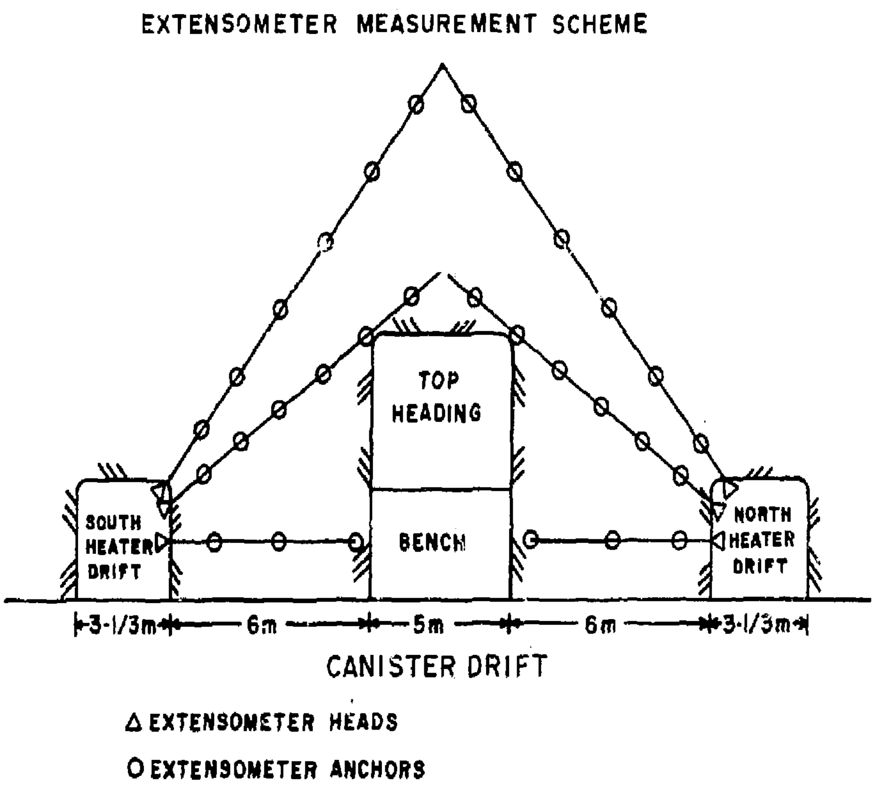
EXTENSOMETER MEASUREMENT SCHEME
TOP
HEADING
BENCH
SOUTH
HEATER
DRIFT
NORTH
HEATER
DRIFT
3-1/3m
6m
5m
6m
3-1/3m
CANISTER DRIFT
△ EXTENSOMETER HEADS
O EXTENSOMETER ANCHORS

Figure 1.

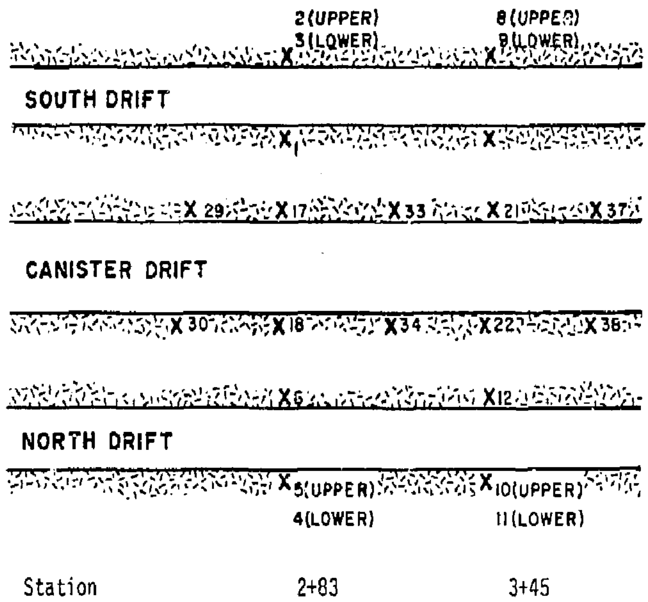

Figure 2. Schematic Drawing of Convergence Point Anchor Locations

TABLE 1

Ext./Anchor #	Original Rod Length	-	Extra Rod Length	-	Distance From Rod Top to Flange	=	Distance From Flange To Anchor Point	
E1-1	144		76.5		2.5		65"	1.65m
-2	168		14.0		2.5		151.5"	3.85m
-3	288		68.0		2.5		217.5"	5.33m
E2-1	144		74.0		2.5		67.5"	1.71m
-2	170		19.0		2.5		148.5"	3.77m
-3	288		53.0		2.5		232.5"	5.91m
-4	336		22.0		2.5		311.5"	7.91m
-5	362		8.5		2.5		351.0"	8.92m
-6	432		23.0		2.5		406.0"	10.33m
E3-1	144		67.5		2.5		74.0"	1.88m
-2	192		1.5		2.5		188.0"	4.78m
-3	332		27.0		2.5		302.5"	7.68m
-4	432		42.5		2.5		387.0"	9.83m
-5	480		7.0		2.5		470.5"	11.95m
-6	576		28.5		2.5		545.0"	13.84m
E4-1	144		75.0		2.5		66.5"	1.69m
-2	204		62.0		2.5		139.5"	3.54m
-3	228		23.5		2.5		204.5"	5.19m
E5-1	144		77.0		2.5		64.5"	1.64m
-2	167.5		23.5		2.5		141.5"	3.59m
-3	263		46.0		2.5		214.5"	5.45m
-4	288		14.0		2.5		271.5"	6.90m
-5	360		21.0		2.5		336.5"	8.55m
-6	432		31.0		2.5		398.5"	10.12m
E6-1	143.5		72.0		2.5		69.0"	1.75m
-2	216		3.5		2.5		210.0"	5.33m
-3	311.5		8.0		2.5		301.0"	7.65m
-4	431		29.5		2.5		399.0"	10.13m
-5	479		5.5		2.5		471.0"	11.96m
-6	575.5		25.5		2.5		547.5"	13.91m
E8-1	144		55.0		2.5		86.5"	2.20m
-2	214		59.0		2.5		152.5"	3.87m
-3	288		71.5		2.5		214.0"	5.44m
E9-1	144		71.5		2.5		70.0"	1.78m
-2	144		0.5		2.5		141.0"	3.58m
-3	288		79.0		2.5		206.5"	5.25m
-4	288		7.0		2.5		278.5"	7.07m
-5	432		83.0		2.5		246.5"	8.80m
-6	432		31.0		2.5		398.5"	10.12m
E10-1	144		70.5		2.5		71.0"	1.80m
-2	262		81.0		2.5		178.5"	4.53m
-3	388		81.5		2.5		304.0"	7.72m
-4	432		48.5		2.5		381.0"	9.68m
-5	552		81.5		2.5		468.0"	11.89m
-6	576		37.5		2.5		636.0"	13.61m
E11-1	144		60.5		2.5		81.0"	2.06m
-2	159		6.5		2.5		150.0"	3.81m
-3	287.5		83.5		2.5		201.5"	5.12m
E12-1	143.5		72.5		2.5		68.5"	1.74m
-2	165.5		5.5		2.5		158.5"	4.03m
-3	287.5		66.0		2.5		219.0"	5.56m
-4	287.0		5.5		2.5		279.0"	7.09m
-5	359.5		21.0		2.5		336.0"	8.53m
-6	432.0		53.5		2.5		376.0"	9.55m
E13-1	143.5		73.0		2.5		68.0"	1.73m
-2	215.0		28.5		2.5		184.0"	4.67m
-3	316.5		10.5		2.5		303.5"	7.71m
-4	431.5		54.5		2.5		374.5"	9.51m
-5	508.0		42.5		2.5		46.3"	11.76m
-6	575.5		50.5		2.5		522.5"	13.27m

1. Rod sections joined, measured and marked

2. Anchors and protective conduits joined and placed around rods

3. Collar stabilizer tube attached to conduit

4. Anchor pressure lines strung and connected to anchors

Placing the instrument in the borehole followed by grouting and setting of the anchor positions was the next step. Due to the length of the instrument, a large crew (minimum 6 persons) is required to move the assembled extensometer and feed it into the borehole. Grouting operations required only a two-man crew. Procedure was as follows:

1. Instrument placed into borehole

2. Anchors positioned by connecting rods and inflated in place

3. Grout tube inserted and collar of hole packed off

4. Grout mix prepared (4 parts water, 2 parts cement, 1 part sand)

5. Collar tube grouted (∿1st meter of hole)

Following curing of the grout, the extensometer head assembly was mounted in place. This involves tensioning of the rods and setup of the measuring system. This task was handled by one person. Procedure is as follows:

1. Rod spring assembly prepared and implaced

2. Rods locked to spring assembly, tensioned and cut to length

3. Transducer mounting and transducers installed and wired

4. Cover plate and calibration screws installed

This completes extensometer assembly. Irregularities associated with this installation are listed below:

<u>Extensometer Irregularities</u>

E2-1 Moved in six inches <u>further</u> from collar than originally specified

E5-6	Anchor struck bottom of hole--i.e., actual hole length was less than believed.
E8-3	Same problem as E5-6.
E9-6	Anchor moved out four inches closer to collar than originally specified.
E10-5,6	Anchors off location due to pinching (jamming) of hydraulic lines during installation.
E11,12,13	Hydraulic tubing bursting at lower pressure levels (~1000 psi) due to inferior grade of tubing, E13-6 burst at 500 psi.

Field Calibration

Extensometer calibrations are *in situ* calibrations involving both manual (portable readout) and remote monitoring of transducer output. The *in situ* calibrations allc for factors of instrument deformation (for example, rod stretch) occuring during displacement measurements. Portable readout readings are hand recorded and serve as both a visual check during calibrations and a calibration for use with portable readout readings taken during the experiments.

Calibrations were performed by raising the head assembly with respect to the upper flange surface of the collar stabilizer tube. Three head lifting screws allowed for this movement. Three machined step blocks were inserted between the stabilizer tube flange and the overhanging lip of the head assembly. Calibrations were performed in steps of 1.00 mm from 10 to 15 millimeters. Following calibration, the head lifting screws were used to place the head at midrange (12 mm).

Since the calibration curves are characteristically slightly nonlinear, actual accuracy of small measurements is expected to be higher than suggested by the standard errors computed over the calibrated 5 mm range.

Field Activity Summary

The following is a summary of the field work performed by Terra Tek in the installation, calibration and monitoring of extensometers for the mine-by experiment. Despite some conflict with other activities at the site installation and calibration of the instrumentation was completed within the scheduled time frame (Terra Tek proposal P78-50). Completion of the rail car room and mining of the top heading for the center canister drift proceeded somewhat faster than originally estimated, however, resulting in some overlap of these activities.

Week 1 (February 7 - February 8)

The instrumentation was delivered to the Lawrence Livermore warehouse in Mercury on the morning of February 8. Access to the forward areas was prevented by poor weather and delays of scheduled nuclear testing.

Week 2 (February 20 - February 23)

Terra Tek field personnel arrived on site on February 20. Arrival on site has been delayed one week by a slow down in drilling operations and the interference of scheduled nuclear testing. The equipment was already underground and assembly of the extensometers was begun in the north heater drift. The extensometers MBI 1, 2, 3, 9 and 10 were assembled and emplaced in their respective boreholes by week's end.

Week 3 (February 26 - March 2)

Terra Tek field personnel returned on site on February 26. Extensometer MBI 8 was assembled and emplaced. All extensometers in the north heater drift (MBI 1, 2, 3, 8, 9 and 10) were then grouted in place. Notification was then received from LLL personnel that due to advancement of the mining schedule the forward stations (MBI 1 thru 6) should be operative as soon as possible.

Lawrence Livermore Laboratory was informed at this time that March 2nd was the earliest possible date for completion of these stations. Arrangements were made with REECO to move drilling equipment in the south heater drift and an assembly area was established. The equipment was moved to the south heater drift and assembly of extensometers MBI 4, 5 and 6 was completed. These extensometers were installed and grouted in place. Measurement heads on MBI 1 thru 6 were installed and wired for manual readout by 5 p.m., March 2nd. At this point, the top heading was approximately 80 feet from the first station. Instructions were left with the LLL site personnel for centering of the instrument heads when hook up to the surface data collection system was completed.

Week 4 (March 5 - March 9)

Terra Tek personnel returned on site on March 5. An assembly area was established on the west end of the south heater drift and assembly of extensometers MBI 11, 12 and 13 was started. Calibration of the forward stations was begun on March 6. As advancement of the top heading was occurring at this time, some data may have been lost. Head assemblies for extensometers MBI 8, 9 and 10 were installed and wired and assembly, installation, and grouting of extensometers MBI 11, 12 and 13 was completed by week's end. Anchor points CA1 thru CA12 were installed and convergence measurements initiated.

Week 5 (March 12 - March 16)

Terra Tek personnel arrived on March 11th to continue convergence point measurements. The head assemblies on extensometers MBI 11, 12 and 13 were installed and wired and extensometers MBI 8 thru 13 were calibrated. The portable extensometer read out unit was altered to operate using the LLL power supplies.

Week 6 (March 19 - March 23)

Extensometers MBI 1 thru 6 were recalibrated. Convergence anchor points were installed in the center drift top heading and measurements begun.

Week 7 (March 26 - March 30)

Extensometers MBI 8, 9 and 10 were recalibrated. Convergence point measurements were continued.

Week 8 (April 2 - April 6)

Convergence point measurements were continued.

Instrument Readings

Records of the data collected by Terra Tek during the mine-by experiment are listed in Tables A through D in the appendices. All data shown was obtained using the portable manual readout unit supplied with the instrumentation. Tables A list the voltage readings recorded along with the respective dates/ times of the readings and the voltage used to power the linear pots. Problems or changes which may have effected the recorded readings are footnoted. Tables B list the displacements (in millimeters) computed from the voltage readings listed in Tables A. Corrections for changes in battery voltage or other offsets were made where possible. The position of the advancing face has also been noted where the position of the face has changed since the last reading. Where more than one face position is noted in the same column more than one advance has occurred between readings. Tables C-1 list the calibration data recorded. The column headings refer to the actual displacement of the instrument head with respect to the collar flange. The table lists the recorded voltages (first line) and the corresponding indicated displacements (second line) computed from the linear regression fit to the actual displacement/ recorded voltage data. With the exception of extensometers 11, 12 and 13 all instruments were recalibrated and these data are also shown. It should be noted that these repeat calibrations were performed between the top heading and benching operations and therefore reflect different instrument voltage zeros. Extensometer 4 was recalibrated twice and these datum (rows 3 and 5 for each sensor) are directly comparable as repeat calibrations. All calibration data was taken in the order shown (left to right). During the repeat calibrations certain displacement steps were repeated to determine instrument precision. Tables C-2 list the statistics determined by a linear regression fit of the recorded data. The sample variance (or standard error) is shown as the variance of the data about the linear regression fit in the displacement axis direction. Tables D list the convergence point readings as change in reading (mm) versus position of the face.

All displacement data (Tables B and D) is plotted versus position of the advancing face in Figure E 1-24 through F 1-6.

Instrument Performance

Performance of the rod extensometers is good to excellent. The calibration statistics indicate instrument readings are generally precise to about 0.02 millimeters (0.001 inch). This is confirmed by the indicated calibration standard errors and repeat readings. The displacement versus face advance curves show good instrument stability when the face is distant from the measurement station with no apparent anchor slippage or creep. The shape of these curves is as expected with the displacement changes increasing to a maximum as the face passes the measurement plane followed by a gradual decrease in measured movement. Extensometers located at similar locations with respect to the opening geometry also compare quite favorably. Very large displacements associated with the number three anchors of extensometers 9 and 10 are probably the result of a large shear zone intersecting the pillar at this point. This zone was observed independently by the shift foreman.

The convergence point measurements were not as accurate as hoped for somewhat obscuring the rather small displacements occurring at these locations. In addition, convergence points located in the center canister drift were subjected to a significant blast damage resulting in a rather discontinuous record. The convergence points located in the north and south drifts however do provide some usable data. The sudden change in these readings (about 1.0 mm) occurring near the end of this data record appears to be a result of instrument malfunction. The instrument failed completely shortly thereafter and was returned for repairs.

NUMERICAL MODELING OF THE SPENT FUEL MINE-BY AND COMPARISON WITH ACTUAL ROCK MASS DISPLACEMENTS

A simple finite element analysis of the spent fuel mine-by was conducted and reported in the previous progress report. A short description of the finite element code used is given. In addition, a simple model of the same problem utilizing a displacement discontinuity code was run as a program check. A comparison of the actual to calculated displacements is given here for a series of computer runs in which rock mass modulus, Poisson's ratio and the ratio and magnitude of horizontal and vertical stresses were varied.

Computer Codes, Methods and Assumptions

The finite element code "DIG" was used to predict rock mass displacements and stresses. This code, constructed by Dr. C.M. St.John of the University of Minnesota was developed specifically for use in modeling mining problems. The code has provision for initial stress, sequential excavation and jointed rock mass behavior. Axisymmetric, plane strain and plane stress problems can be modeled.

The displacement discontinuity code "TWODI", written by Dr. Steven L. Crouch, University of Minnesota, was used as a comparison to the computed displacements and stresses from the DIG code. The code allows for the analysis of two dimensional, linear elastic, plane strain problems in infinite or semi-infinite bodies. Only the boundaries of an excavation need be discretized by a number of displacement discontinuities. The code is therefore efficient and simple to use.

A. Methods and Assumptions.

For this simple analysis, the mining of the north and south heater drifts and the heading and bench of the spent fuel drift were idealized as a problem in plane strain. Figures 3 a-c illustrate the idealization of the three tunnel system. Since the three tunnels are long in comparison with the width of the area of interest, and since the displacements were measured within the central section of the tunnel system, the assumption of plane strain is a reasonable one. The calculated displacements and stresses are not representative, however, of those which occur near the ends of the system where the three tunnels converge.

B. Boundary Conditions.

The mining was further considered to be symmetrical about the vertical centerline of the spent fuel storage drift. The horizontal displacements are therefore fixed along the vertical symmetry line. The vertical and horizontal boundaries of the finite element mesh (Figure 4) were extended to 30.5 meters (100 feet) beyond the centerline of the spent fuel storage drift to avoid any boundary effects. The horizontal boundaries were fixed in the vertical direction, and vertical boundaries fixed in the horizontal direction prior to application of initial stresses. Triangular and quadrilateral elements were used to model the rock mass.

The boundary conditions of the displacement discontinuity code were identical, except that the rock mass was considered to be infinite in extent. This idealization is illustrated in Figure 5.

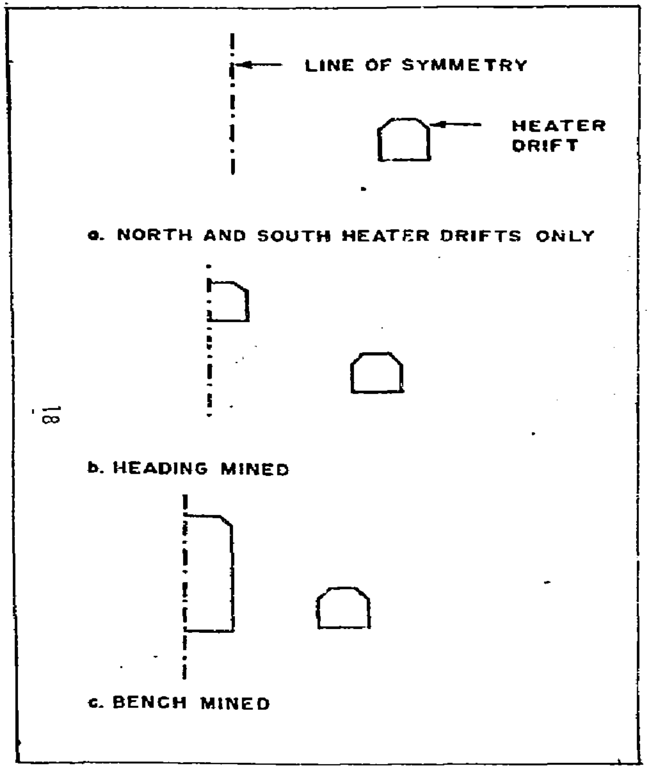

Figure 3. Mining of heater spent fuel storage drifts.

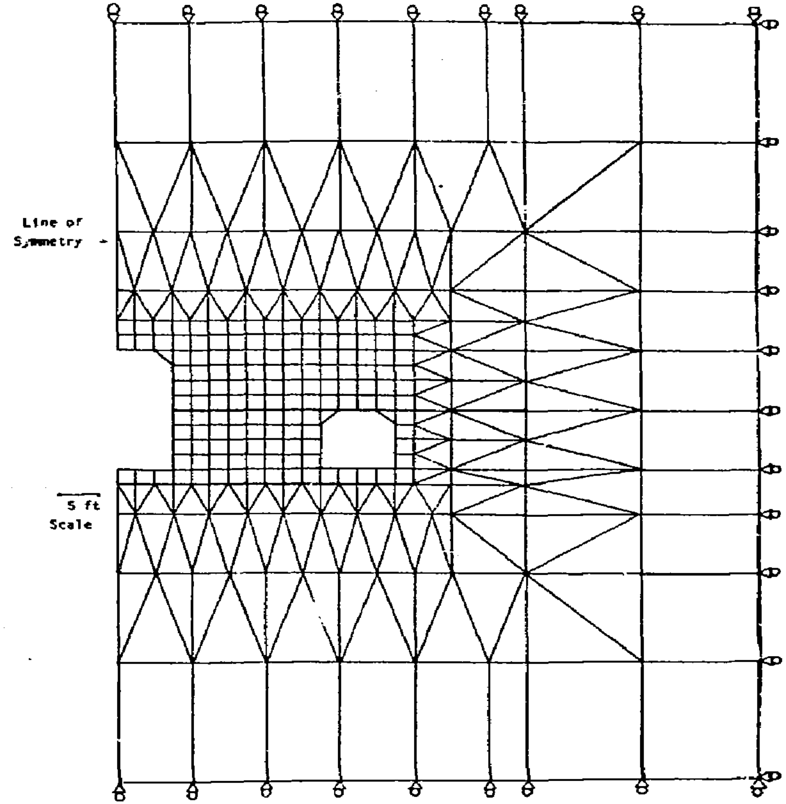

Figure 4. Finite Element Mesh used to Model the Mine-by.

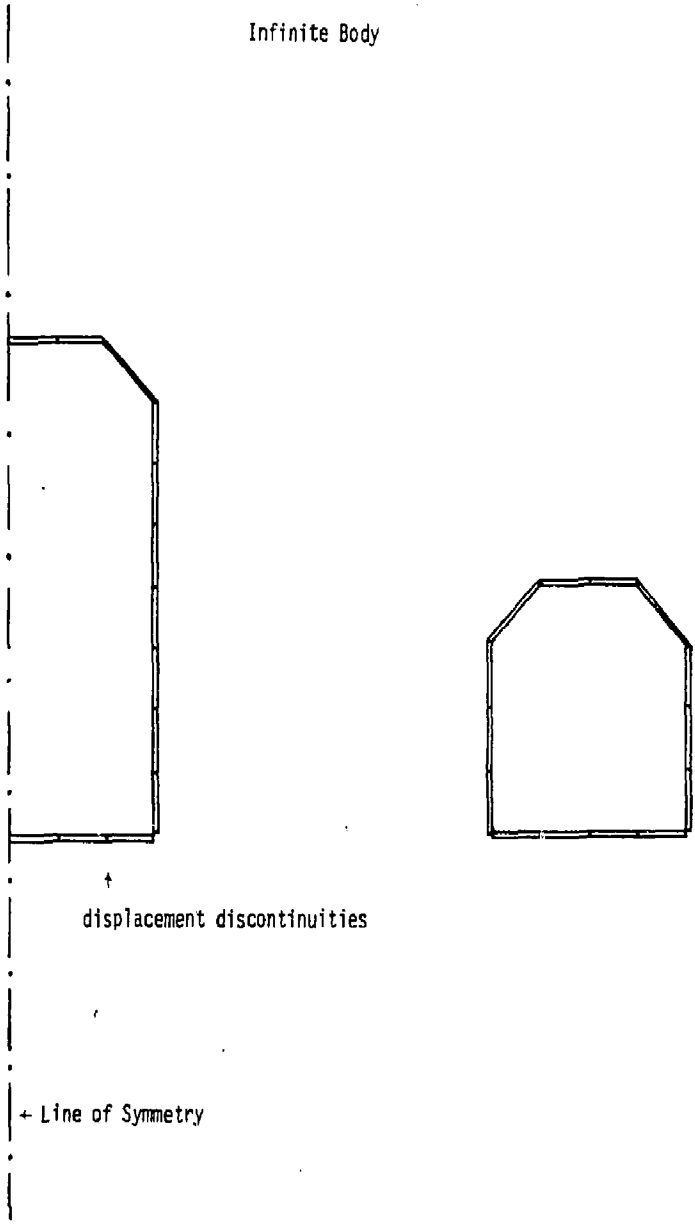

Figure 5. Idealization of the Mine-by for the Displacement Discontinuity Model.

C. Initial Conditions.

The initial stress state in DIG is applied at each element centroid prior to mining. Table 2 shows the variation of *in situ* stresses used in the modeling runs. Table 5 further defines the parameters varied during these runs.

TABLE 2

VARIATION OF *IN SITU* STRESSES*

σvert (psi)	σhoriz (psi)
1500	1200
1200	1500

The horizontal and vertical stresses were assumed to be the principal stresses.

D. Material Properties.

The rock mass was considered to be a homogeneous linear elastic medium with properties given in Table 3. Initial runs assumed a single modulus for the entire rock mass. Later runs were made in which the modulus of the pillar between the heater and spent fuel drifts was reduced to simulate a zone of blast damage or natural destressing around the openings.

* The second stress state given below more closely represents the stresses as measured by the USGS.

TABLE 3

MATERIAL PROPERTIES
USED IN MODEL RUNS

Young's Modulus Rock Mass Er (psi)	Young's Modulus Pillar Ep (psi)	Poisson's Ratio Rock Mass ν_r	Poisson's Ratio Pillar ν_p
5×10^6		.2	
5×10^6		.25	
5×10^6	1×10^6	.2	.25

Table 4 gives a listing of all of the runs that were made with both DIG and TWODI.

TABLE 4

PARAMETERS VARIED FOR MODEL RUNS

Run	E_r	E_p	ν_r	ν_p	σ_H	σ_V	Codes Used
1	$5x10^6$		.2		1200	1500	DIG TWODI
2	$5x10^6$		.2		1500	1200	DIG TWODI
3	$5x10^6$		.25		1200	1500	DIG
4	$.5x10^6$		.25		1200	1500	DIG
5	$5x10^6$	$1x10^6$	.2	.25	1200	1500	DIG
6	$5x10^6$	$1x10^6$	.2	.25	1500	1200	DIG

Results of Modeling

Both codes used have been compared to analytical solutions and the results have been documented (St. John, 1972; Crouch, 1976). A comparison of the results of the two codes was made for the case of the first mining step (i.e., heater drifts only mined) with a biaxial loading of $\sigma_{vertical}$ = -216,000 psf (-1500 psi) and $\sigma_{horizontal}$ = -172,800 psf (-1200 psi). Table 5 gives a comparison of the X- and Y- displacements as calculated by DIG and TWODI at the tunnel rib and crown midplanes. The agreement is quite good, and is a function of the degree of discretization of the tunnel boundaries. It was seen (Figure 5) that quite a coarse discretization of the boundary was used in the displacement discontinuity run.

TABLE 5

COMPARISON OF RESULTS OF THE FINITE ELEMENT
AND DISPLACEMENT DISCONTINUITY METHODS

Code	θ (deg)*	Ux (ft)	Uy (ft)	Comments
DIG	0	-.0016	-.0002	The displacements are given at the drift boundary
TWODI	0	-.0019	-.00014	
DIG	90^0	.00007	-.0023	
TWODI	90^0	.00004	-.0026	

* θ = 0 is displacement at tunnel rib midplane; θ = 90^0 is displacement at tunnel crown midplane.

A. Displacement Calculations.

The relative displacements of anchor to collar were calculated from the computer output in the following manner:

1. The north and south heater drifts were mined, and new nodal coordinates calculated from initial nodal coordinates and nodal displacements. These new coordinates are considered the starting coordinates for further relative anchor displacement calculations.

2. As the heading and bench are mined, new nodal coordinates are calculated. The distances between the nodes along the length of the rod and the collar node are then calculated. This distance is then subtracted from the distances between nodes calculated after mining of the heater drifts. The change in distance is therefore the relative displacement between anchor and collar and is analogous to the displacement as measured from the extensometers.

B. Comparison of Actual to Theoretical Displacements

Figures 6 to 11 show a comparison of the measured and predicted displacements as a function of rod length for the 0^0, 33^0 and 50^0 extensometers during the heading and benching operations. The theoretical displacements were calculated on the basis of a rock mass modulus of $5x10^6$ psi, Poisson's ratio of .2, vertical stress of 1500 psi and horizontal stress of 1200 psi. As seen in Figures 6 and 7, the displacements as determined from the horizontal extensometers is consistent between all four extensometer locations. There is some variation in magnitude, however all anchors show a convergence of anchor and collar, or a net decrease in pillar width. In addition, the magnitude of these displacements are approximately 4 to 6 times that predicted. The predicted displacements, however, show a divergence of anchor and collar, and thus a net increase in pillar width.

The 33^0 extensometers show a trend much closer to the calculated values. Figures 8 and 9 show the relative anchor displacements for all 33^0 extensometers as a function of distance from the hole collar for both heading and benching. With the exception of one anchor, all displacements for extensometer E2 are less than predicted for the heading operation. All other anchors show greater displacements than predicted, with extensometer E5 providing the best fit, with actual displacements approximately twice the predicted. The agreement between actual and predicted improves somewhat during the benching operation. Figure 9 indicates that the ratio of actual to predicted displacements is nearly one for extensometers E2 and E5.

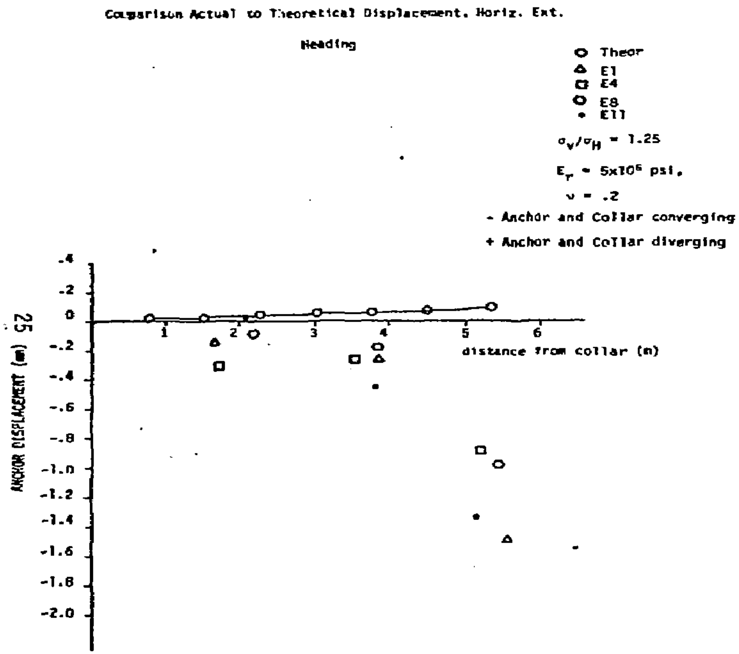

Figure 6. Actual and Predicted Displacement during Mining of the Heading, Horizontal Extensometers.

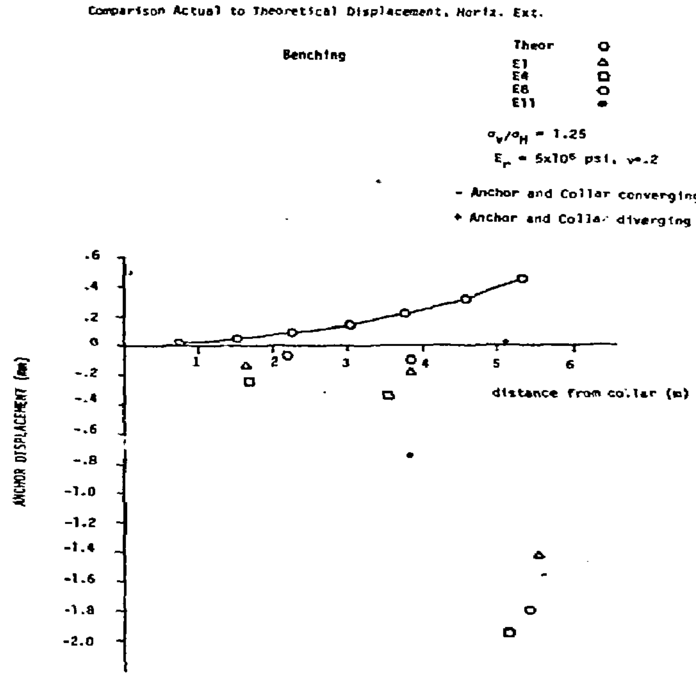

Figure 7. Actual and Predicted Displacement during mining of the Bench, Horizontal Extensometers

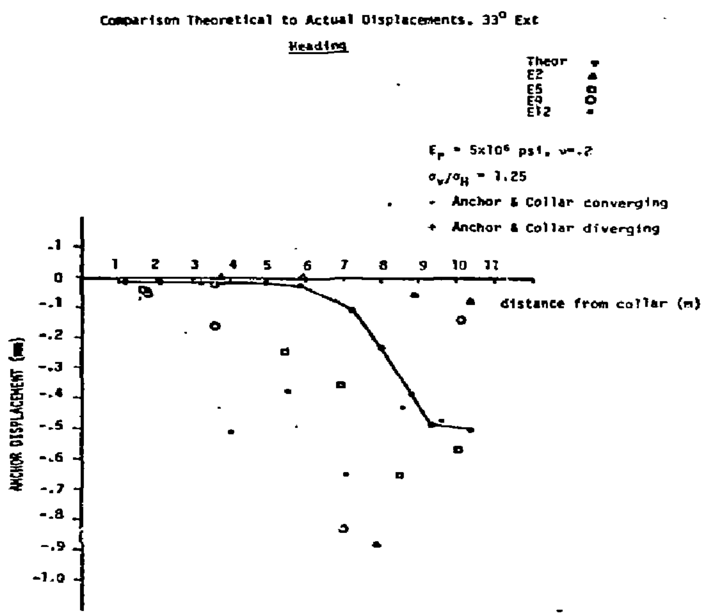

Figure 8. Actual and Predicted Displacement during Mining of the Heading, 33° Extensometers.

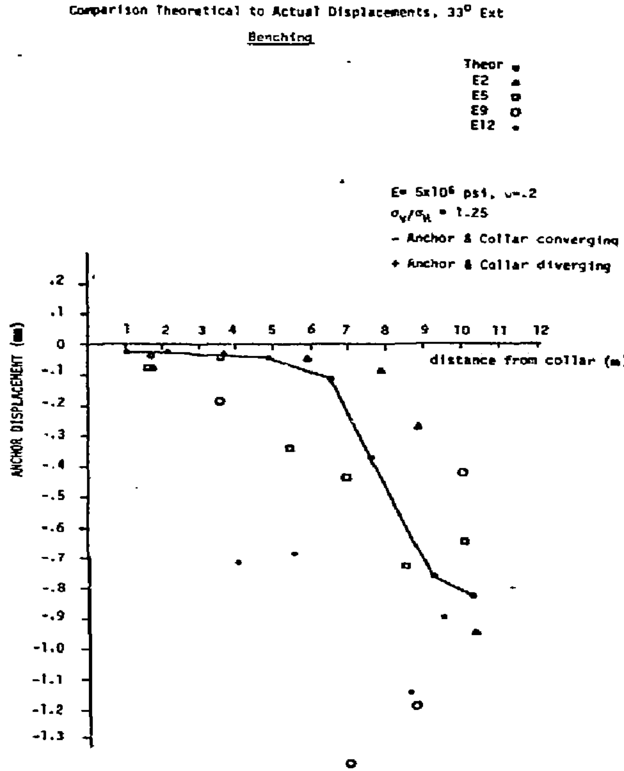

Figure 9. Actual and Predicted Displacement during Mining of the Bench, 33° Extensometers.

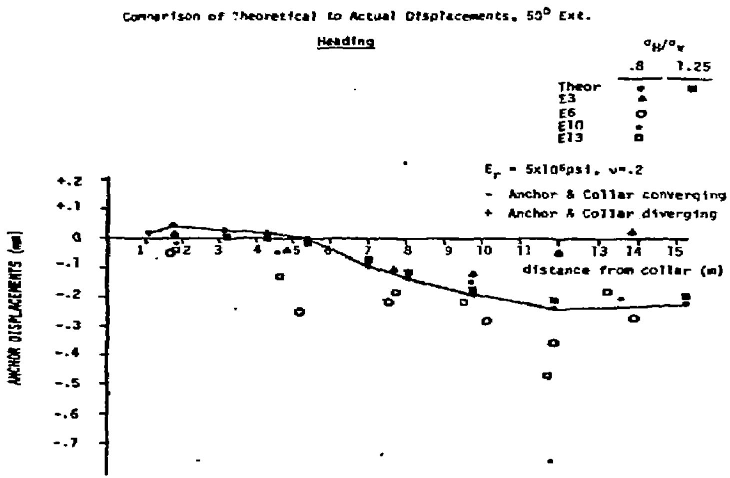

Figure 10. Actual and Predicted Displacements during mining of the Heading, 50° Extensometers.

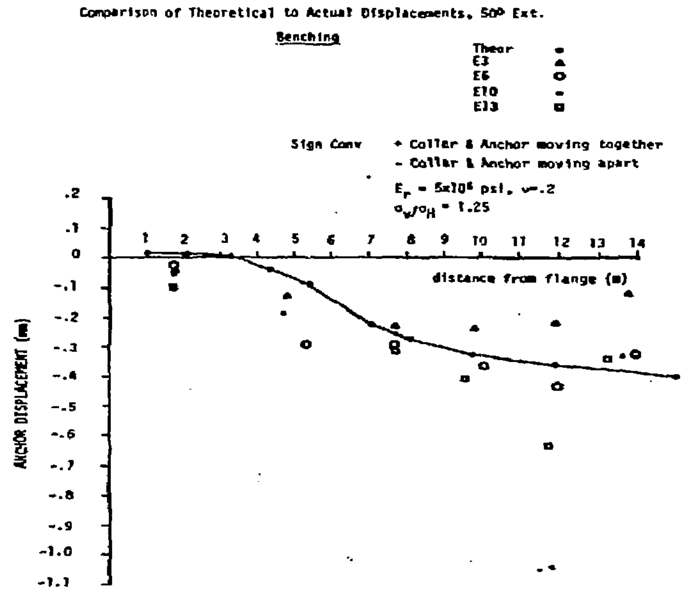

Figure 11. Actual and Predicted Displacements after Mining of the Bench, 50° Extensometers.

In general, the back two extensometers, E9 and E12, show more erratic behavior and greater displacements. This might be attributed to the fact that the rock is more highly fractured in this section (Schrauf, 1979). However, by comparison with the less erratic extensometers (E2 and E5), quite good agreement is obtained after the benching operation.

Figures 10 and 11 show the actual and predicted displacements after the heading and benching operations for all 50^0 extensometers. For comparison purposes, the case of the horizontal stress of 1500 psi and vertical stress of 1200 psi is given, since this appears to better approximate recent stress measurements made at the Climax Stock (Patrick, 1979). Figure 10 indicates an excellent agreement of actual and theoretical displacements after heading operations. The scatter of the actual measurements is much less than the 33^0 extensometers, with the exception of the longer rods in E3 and E10. It is seen that a stress state of $\sigma_H/\sigma_v = 1.25$ makes little difference in the calculated displacements. After benching (Figure 11), the scatter of the actual displacements decreases further. Only anchor 5 and anchor 6 on extensometers E10 and E3, respectively, show divergence from the grouped data. From these data, the following conclusions can be drawn:

1. The two upper extensometers show generally good agreement with the predicted data, and indicate an in situ rock mass modulus of $3\text{-}5 \times 10^6$ psi.
2. The data from all extensometer anchors show a general consistency, thus lending credence to their results. Displacements at some anchor locations varies widely, indicating possible structural control of the displacements.

3. The horizontal extensometers indicate displacements in the opposite direction as predicted with a magnitude of 3 to 5 times the predicted levels.

The convergence measurements help little in sorting out the horizontal displacements. The measurements show little closure of the heater drifts (Figures F1 to F6). The measurements across all drifts show varying results. Station 3+42 indicates a convergence of the heater drifts of approximately 1.0 mm, whereas station 2+80 shows a divergence of the drifts of approximately 1.0 mm. Assuming the reliability of these measurements, structural control of the convergence is indicated.

The stress change as measured by the IRAD gages indicate significant reduction in the vertical compression across the pillar as the heading is mined (Patrick, 1979). As seen in Figure 12, the finite element model indicates an increase in vertical compression across the pillar between the spent fuel and heater drift. The reduction in the actual vertical stress induced across the pillar (as measured by the IRAD gages) indicates that a stress arch has formed around the openings, thus unloading the pillar. The unloading of the pillar, resulting in a relaxation and a decrease in pillar width, could account for the anomalous horizontal displacements. The unloading of the pillar and the formation of an arch around the openings could be the result of several factors including:

1. Reduction in modulus of the pillar due to blasting damage and/or natural destressing by fracturing due to the concentration of loads caused by the small pillar dimensions.

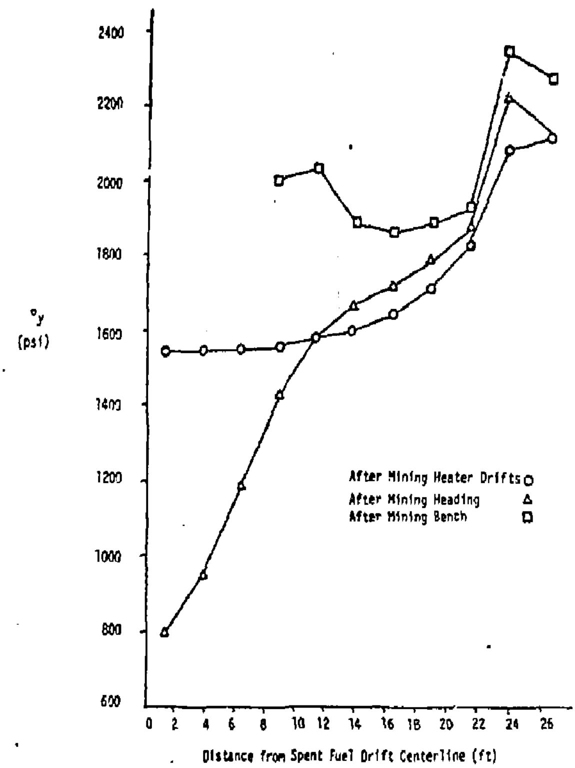

Figure 12. Vertical stress across pillar centerline during mining of the Spent Fuel drift.

2. Slip along joints and thus block motion in the pillar, due to its small dimension in relation to the dimensions of the drifts. As a result of block motion, a stable stress arch could be formed around the openings, thus unloading the pillar.

To examine the possibility of a reduced rock mass modulus for the pillar resulting in an arching effect, several computer runs were made with the DIG code in which the pillar modulus was reduced to $1x10^6$ psi and a Poisson's ratio of .25 (Figure 13). As seen in Figures 14 to 19, the net effect of the reduction is to increase the magnitude of the displacements for all extensometers during the heading and benching operations. Figure 20 indicates that the vertical load in the pillar has been reduced, but not by a significant amount. The assumption of a simple reduction in modulus of the pillar therefore does not explain the anomalous horizontal displacements.

Recent work by Voegele (1978) and Barton (1979) has shown how jointing can control displacements and stresses in the vicinity of underground workings. These studies, in which large motion block models (both numerical and physical) are used, indicate that the geologic structure can control both the magnitude and direction of displacements, particularly in the rock mass adjoining multiple openings. In the case of the spent fuel mine-by, the pillars between the spent fuel storage and heater drifts are quite small, approximately one diameter of the spent fuel drift. It is common mining practice to maintain pillars between drifts in, for example, lane and pillar systems, of at least two and normally three tunnel diameters. The spacing allows a confined "core" of the pillar which allows the rock to behave in an

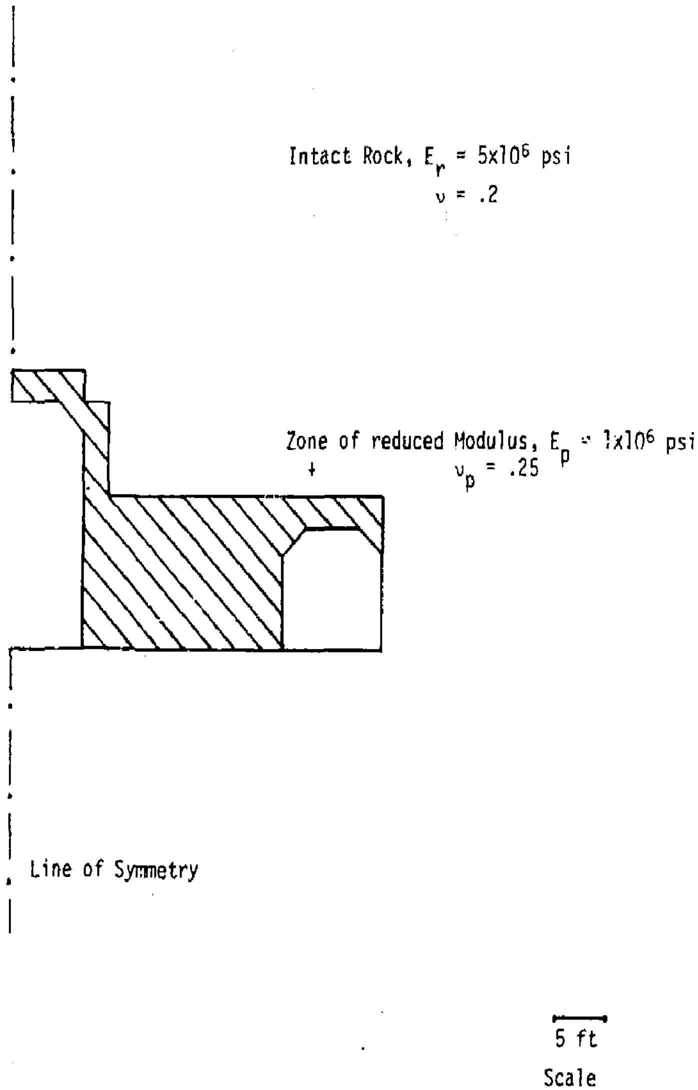

Figure 13. Zone of Reduction in pillar modulus used in the finite element models.

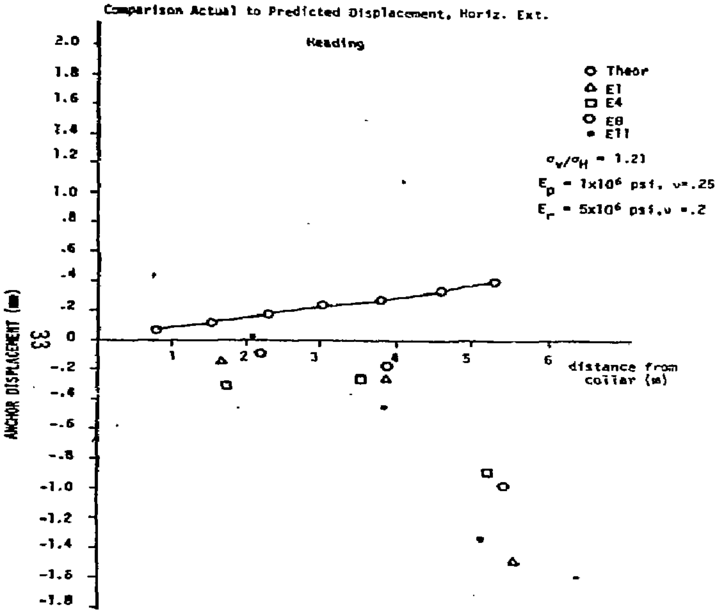

Figure 14. Actual and Predicted Displacements during Mining of the Heading, Horizontal Extensometers.

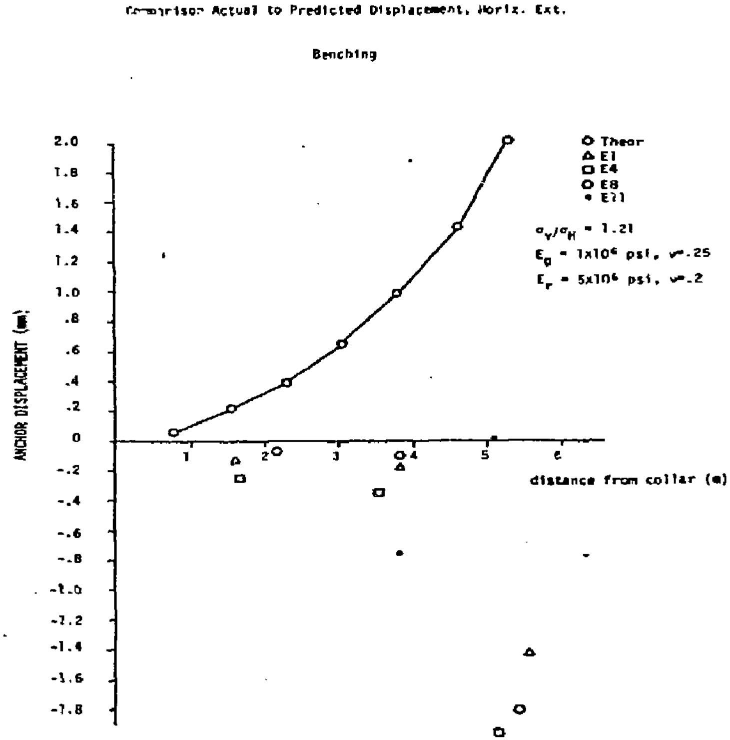

Figure 15. Actual and Predicted Displacements during Mining of Bench, Horizontal Extensometers.

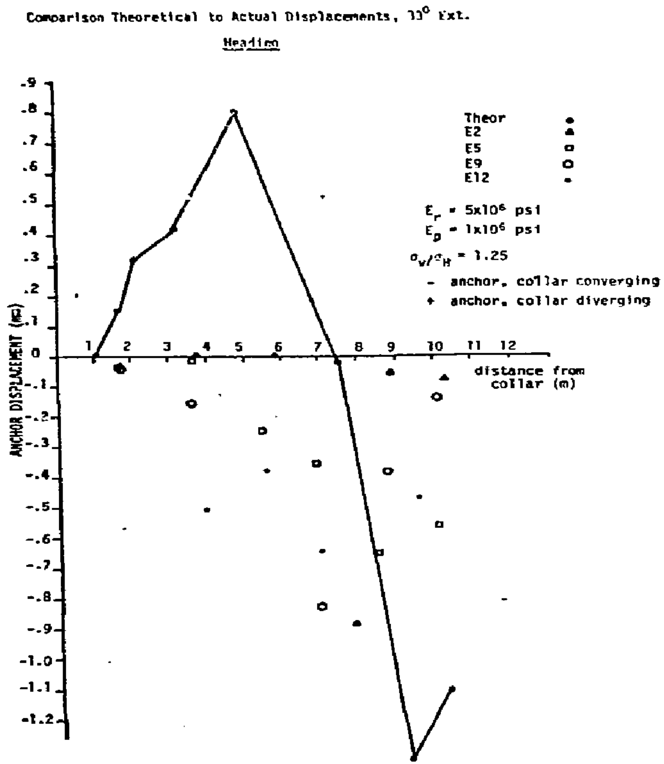

Figure 16. Actual and Predicted Displacements during Mining of Heading, 33° Extensometers.

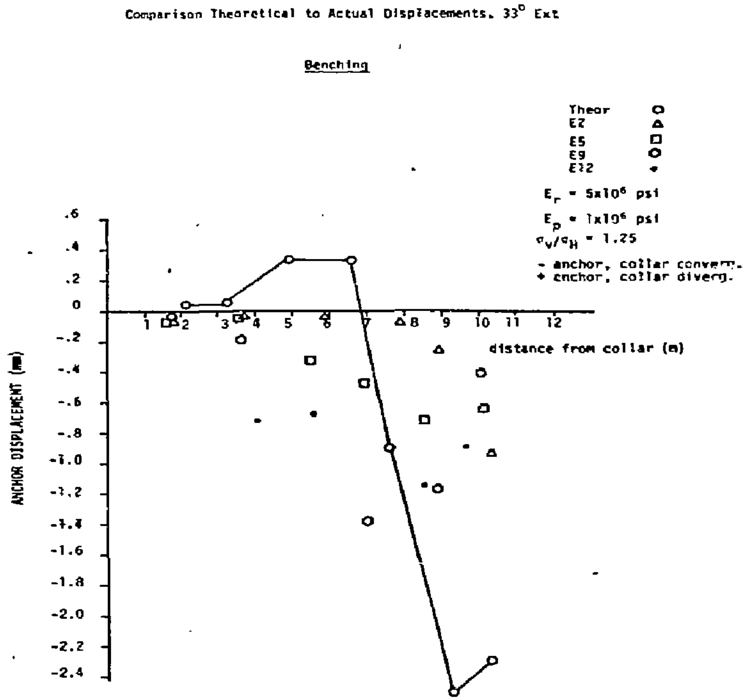

Figure 17. Actual and Predicted Displacements during Mining of Bench, 33° Extensometers.

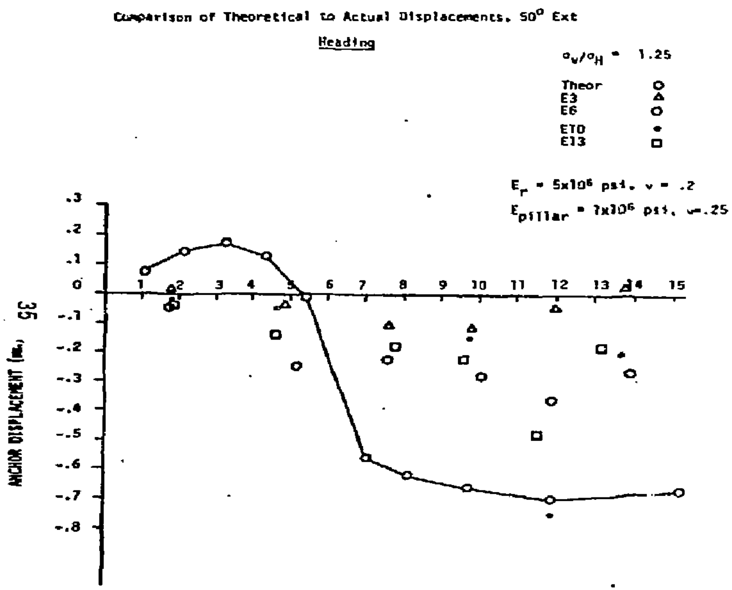

Figure 18. Actual and Predicted Displacements during Mining of the Heading, 50° Extensometers.

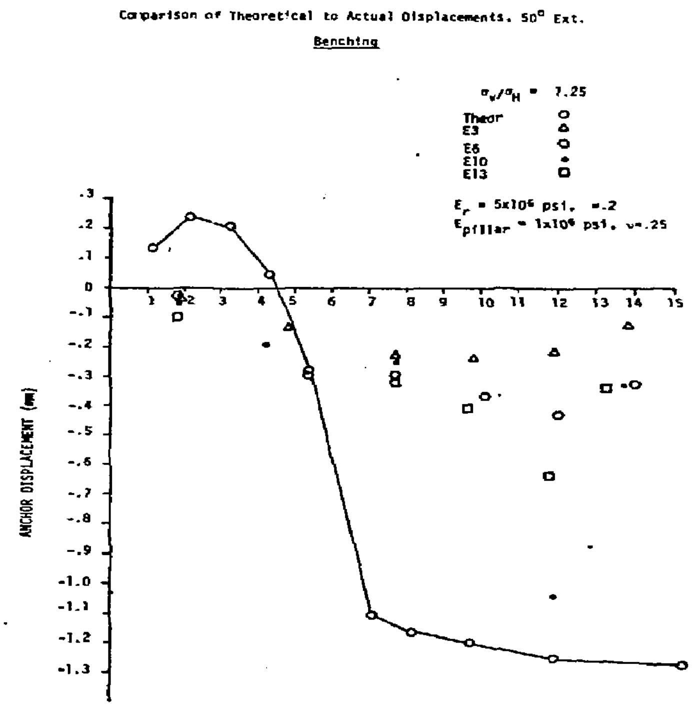

Figure 19. Actual and Predicted Displacements during Mining of the Bench, 50° Extensometers.

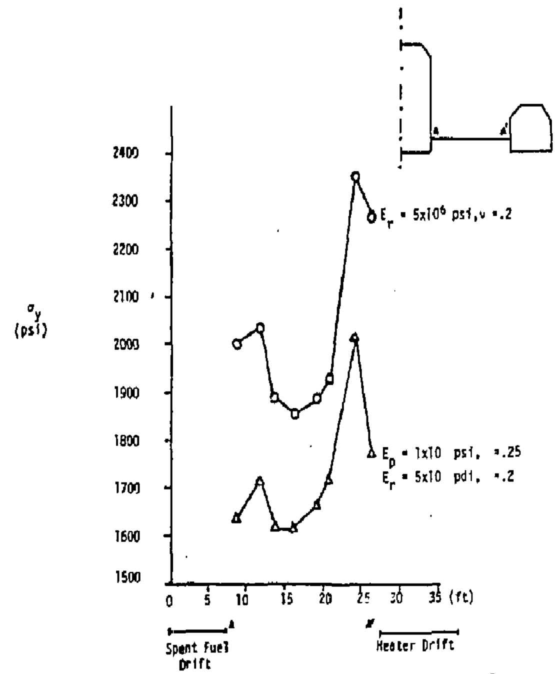

Figure 20. Plot of Vertical Stress (Total) Along Line A-A' After All Mining for Case of Single Modulus and Reduced Pillar Modulus.

elastic manner. As pillar dimensions are decreased, the confinement is reduced. The geologic structure thus becomes more important and can control the resulting rock mass response. Observations which might support these ideas to explain the mine-by displacements are the following:

1. Only the horizontal extensometers which are entirely within the pillar show the anomalous behavior. The upper extensometers, which show reasonable behavior, are not located within the pillar.
2. The IRAD gages show a large decrease in compression across the pillar. This indicates an unloading of the pillar and formation of a stress arch around the openings.
3. During the mining of the heading and bench, block motion and some slabbing in the heater drifts was observed (Schrauf, 1979).
4. Larger displacements were generally recorded at the back stations where the rock mass is more highly jointed.

It would appear that some work should be done to try and correlate the intensity and attitude of jointing to the observed displacements. If time and/or money permits, the geometry of the jointing and mine openings might be modeled by a large displacement block model as is currently in use at the University of Minnesota (Voegele, 1978).

CONCLUSIONS

The extensometers performed well during the mine-by. Results have shown good consistency between anchors at all extensometer locations. Blasting vibration during the mining of the spent fuel drift has appeared to have little effect on instrument performance. Field calibration of the instruments show excellent repeatability.

Convergence measurements have shown varying results. Closure measurements in the heater drifts indicate small displacements. Convergence measurements in the spent fuel drift yielded poor results due to blast damage.

Comparison of measured to predicted displacements have shown the following:

1. The displacements from the 33^0 and 50^0 extensometers compare well with those calculated from a simple continuum finite element model. The rock mass modulus for best fit of the data appears to be approximately $3\text{-}5\times10^6$ psi. Runs made with ratios of horizontal to vertical stress of .8 and 1.25 make little difference in the calculated relative extensometer displacements. It is interesting to note that the agreement of actual to theoretical displacements becomes worse as the extensometer nears the pillar between drifts (i.e., the 50^0 shows best agreement, 33^0 next, and horizontal worst).

2. The horizontal extensometers indicate a convergence of anchor and collar rather than the divergence as predicted. In addition, the IRAD gages indicate a large reduction in compression across the pillar, unlike the model runs which indicate an increase in

compression. Thus, it would appear that the pillar is unloading. This unloading is consistent with the anomalous horizontal displacements.

3. It would appear that the unloading is a result of the formation of a stress arch around the openings. The arch formation could be a result of sliding along joint surfaces due to close proximity of the heater and spent fuel drifts, and the small dimensions of the pillar with respect to the openings dimensions.

APPENDIX A

EXTENSOMETER VOLTAGE READINGS

Tables A

Voltage Readings (volts)

Instrument I.D.	3-6 15:30	3-6 17:00	3-7 09:00	3-7 11:30	3-7 15:00	3-8 10:50	3-8 12:00	3-9 07:30	3-9 10:49	3-12 14:50	3-12 18:36	3-13- 06:00	3-13 13:51	3-14 22:39
E1-1	5.017	5.017	5.016	5.014	5.014	4.608	4.608	4.584		4.568	4.564	4.559	4.557	4.556
-2	4.936	4.944	4.933	5.004	5.002	4.570	4.589	4.515		4.436	4.411	4.476*	4.471	4.470
-3	5.010	5.030	5.049	5.059	5.058	5.304	5.303	5.163		4.927	4.907	4.859	4.757	4.731
E2-1		5.003	5.003	5.004	5.004	4.989	4.988	4.978		4.977	4.973	4.973	4.973	4.972
-2		5.088	5.087	5.083	5.083	5.054	5.054	5.043		5.065	-----	5.052	5.049	5.033
-3		5.031	5.029	5.033	5.033	4.996	4.996	4.994		4.997	4.996	4.993	4.994	4.991
-4		5.034	5.036	5.041	5.041	5.003	5.003	4.846		4.673	4.671	4.669	4.668	4.669
-5		5.071	5.072	5.078	5.078	5.044	5.043	5.052		5.014	5.015	5.007	5.006	5.012
-6		5.029	5.023	5.013	5.013	4.967	4.967	4.969		4.934	4.927	4.922	4.922	4.927
E3-1		4.991	4.989	4.987	4.988				4.966	4.968	4.963	4.966	4.965	4.964
-2		5.009	5.010	5.012	5.012				4.977	4.961	4.955	4.958	4.959	4.957
-3		4.994	4.993	5.001	5.001				4.965	4.934	4.930	4.928	4.928	4.926
-4		5.040	5.039	5.044	5.043				5.013	4.977	4.972	4.971	4.969	4.968
-5		5.034	5.032	5.039	5.039				4.995	4.991	4.985	4.986	4.983	4.978
-6		5.090	5.093	5.101	5.103				4.928	4.947	4.940	4.939	4.941	4.940
Battery Voltage	9.994	-----	9.993	9.993	9.993	9.995	9.994	9.994	-----	9.994	9.993	9.994	9.993	9.994
						↑ New Zero (E1,E2) Following Calibration and 2 blasts.			↑ New Zero (E3) Following Calibration and 4 blasts.					

* loose connection - retightened

Voltage Readings (volts)

Instrument I.D.	3-15 08:45	3-16 10:01	3-16 15:37	3-20 09:51	3-21 08:48	3-22 19:42	3-22 20:25	3-23	3-23 12:38	3-23 13:15	3-23 14:00	3-26 10:05	3-27 14:18	3-29 13:13
E1-1	4.557	4.557	4.539	4.539	4.539	4.539	4.554					4.553	4.554	4.554
-2	4.471	4.471	4.454	4.455	4.455	4.456	4.478					4.477	4.479	4.487
-3	4.727	4.727	4.709	4.712	4.713	4.801[2]	4.911					4.907	4.908	4.897
E2-1	4.973	4.973	4.954	4.954	4.954	4.954	4.953	4.973	4.969			4.967	4.967	4.971
-2	5.052	5.052	5.033	5.034	5.034	5.034	5.034	5.051	5.046			5.043	5.044	5.052
-3	4.995	4.997	4.979	4.980	4.980	4.979	4.979	4.993	4.998			4.996	4.997	5.000
-4	4.674	4.676	4.659	4.661	4.661	4.660	4.661	4.685	4.683			4.680	4.681	4.684
-5	5.021	5.021	5.003	5.007	5.007	5.007	5.007	5.026	5.030			5.028	5.031	5.037
-6	4.935	4.935	4.917	4.919	4.919	4.920	4.919	4.998	4.989			4.986	4.988	4.953
E3-1	4.965	4.964	4.946	4.945	4.945	4.945				4.942	4.951	4.950	4.950	4.947
-2	4.959	4.959	4.940	4.938	4.938	4.938				4.932	4.939	4.936	4.937	4.928
-3	4.927	4.927	4.908	4.909	4.909	4.908				4.905	4.927	4.925	4.926	4.901
-4	4.968	4.967	4.949	4.948	4.948	4.947				4.943	4.960	4.957	4.958	4.943
-5	4.977	4.978	4.959	4.959	4.959	4.959				4.958	5.006	5.004	5.005	4.961
-6	4.942	4.941	4.923	4.923	4.923	4.923				4.922	4.964	4.962	4.962	4.925
Battery Voltage	9.994	9.993	9.966[1]	-----	-----	9.968	9.968	9.968	-----	-----	-----	-----	-----	-----
							↑ (E1)	↑ (E2)			↑ (E3)			

New Zeros Following Calibration

[1] Power supply switched from portable readout to L^3 system.

[2] Pot loose - rezeroed and tightened.

Voltage Readings (volts)

Instrument I.D.	3-30 10:30	4-2 12:17	4-3 11:40	4-4 01:26	4-4 21:21	4-6 00:16	4-6 06:11	4-10 11:27
E1-1	4.556	4.554	4.561	4.562	4.562	4.563	4.562	4.559
-2	4.490	4.489	4.516	4.516	4.521	4.522	4.523	4.522
-3	4.901	4.899	4.932	4.932	4.942	4.942	4.936	4.934
E2-1	4.971	4.969	4.968	4.968	4.966	4.968	4.968	4.965
-2	5.051	5.049	5.046	5.046	5.044	5.045	5.043	5.041
-3	5.000	4.998	4.982	4.982	4.982	4.982	4.984	4.982
-4	4.685	4.684	4.667	4.668	4.668	4.668	4.671	4.667
-5	5.040	5.039	5.019	5.019	5.023	5.023	5.025	5.024
-6	4.955	4.953	4.938	4.938	4.937	4.938	4.936	4.933
E3-1	4.947	4.945	4.948	4.949	4.949	4.950	4.949	4.947
-2	4.928	4.926	4.919	4.920	4.920	4.921	4.920	4.918
-3	4.900	4.899	4.883	4.889	4.891	4.892	4.893	4.890
-4	4.944	4.941	4.926	4.927	4.927	4.927	4.929	4.928
-5	4.961	4.961	4.946	4.946	4.950	4.951	4.947	4.946
-6	4.924	4.923	4.914	4.915	4.913	4.915	4.914	4.912
Battery Voltage	-----	9.968	9.969	9.970	9.968	9.970	9.969	9.968

Voltage Readings (volts)

Instrument I.D.	3-6 14:30	3-6 17:40	3-7 08:40	3-7 10:30	3-7 11:30	3-7 13:40	3-7 14:45	3-8 09:00	3-8 13:00	3-8 15:00	3-9 08:00	3-12 15:15	3-12 18:22	3-13 05:23
E4-1	5.076	5.075	5.078	5.141	5.137			5.135	5.135	5.134	5.118	5.084	5.048	5.039
-2	5.011	5.012	5.012	5.020	5.013			5.015	5.015	5.015	5.002	4.974	4.941	4.935
-3	5.088	5.081	5.080	5.117	5.118			5.118	5.117	5.117	4.963	4.823	4.796	4.789
E5-1	4.842	4.844	4.843			4.868		4.866	4.867	4.867	4.862	4.858	4.853	4.852
-2	4.836	4.839	4.838			4.861		4.855	4.855	4.856	4.846	4.858	4.856	4.854
-3	4.808	4.811	4.811			4.830		4.827	4.826	4.827	4.763	4.755	4.745	4.741
-4	4.799	4.798	4.797			4.810		4.804	4.804	4.804	4.742	4.709	4.688	4.681
-5	4.728	4.715	4.715			4.729		4.721	4.720	4.720	4.626	4.507	4.494	4.487
-6	4.892	4.882	4.882			4.893		4.882	4.882	4.882	4.805	4.725	4.715	4.704
E6-1	4.901	4.902	4.901		4.902		4.879	4.879	4.877	4.878	4.873	4.870	4.865	4.861
-2	4.830	4.832	4.834		4.833		4.801	4.787	4.786	4.787	4.771	4.722	4.711	4.708
-3	4.861	4.862	4.861		4.862		4.824	4.818	4.818	4.817	4.802	4.766	4.754	4.744
-4	4.790	4.791	4.794		4.795		4.780	4.761	4.760	4.760	4.744	4.679	4.685	4.676
-5	4.834	4.834	4.833		4.833		4.826	4.807	4.806	4.806	4.770	4.732	4.725	4.709
-6	4.832	4.832	4.831		4.834		4.819	4.807	4.807	4.807	4.785	4.739	4.732	4.728
Battery Voltage	9.995	9.994	9.991	9.993	9.993	9.993	9.993	9.995	9.994	9.994	9.994	9.994	9.993	9.994
				↑ (E4)		↑ (E5)	↑ (E6)							

Calibration Rezeros

Voltage Readings (volts)

Instrument I.D.	3-13 14:22	3-14 22:48	3-15 08:31	3-16 09:48	3-16 15:18	3-20 09:29	3-21 09:11	3-22 13:15	3-22 13:20	3-22 14:14	3-22 18:11	3-22 18:50	3-22 20:00	3-26 10:32
E4-1	5.028	5.026	5.024	5.021	5.014	5.016	5.016	5.015		5.094	5.092			5.090
-2	4.921	4.921	4.922	4.920	4.914	4.915	4.915	4.914		5.004	5.002			4.998
-3	4.781	4.782	4.786	4.783	4.776	4.782	4.782	4.782		4.828	4.822			4.819
E5-1	4.854	4.852	4.852	4.851	4.845	4.845	4.846		4.862			4.866		4.861
-2	4.851	4.850	4.851	4.849	4.844	4.845	4.846		4.862			4.869		4.864
-3	4.739	4.738	4.738	4.736	4.731	4.732	4.733		4.748			4.755		4.749
-4	4.677	4.677	4.678	4.676	4.671	4.673	4.674		4.689			4.691		4.689
-5	4.485	4.484	4.487	4.485	4.479	4.481	4.481		4.495			4.495		4.497
-6	4.704	4.704	4.706	4.705	4.700	4.701	4.701		4.716			4.716		4.720
E6-1	4.860	4.859	4.860	4.858	4.853	4.854	4.853	4.853					4.840	4.835
-2	4.706	4.705	4.705	4.704	4.709	4.697	4.697	4.697					4.723	4.725
-3	4.742	4.739	4.739	4.737	4.732	4.733	4.732	4.732					4.766	4.762
-4	4.671	4.668	4.666	4.667	4.662	4.663	4.662	4.662					4.686	4.687
-5	4.705	4.704	4.695	4.694	4.689	4.690	4.689	4.689					4.706	4.722
-6	4.722	4.719	4.717	4.717	4.711	4.712	4.712	4.711					4.734	4.734
Battery Voltage	9.994	9.994	9.994	9.993	9.995[1]			9.995	10.032[2]		10.029	10.031		
										(E4)	(E4)	(E5)	(E6)	
										Rezeros after Recalibration				

1 Power supply switched from portable readout to L^3 system.

2 Fuse changed and so did power supply voltage.

Voltage Readings (volts)

Instrument I.D.	3-27 14:00	3-29 13:26	3-30 10:44	4-2 12:49	4-2 13:00	4-3 11:52	4-3 12:10	4-4 01:15	4-4 22:22	4-4 22:32	4-6 00:38	4-6 06:31	4-10 12:04
E4-1	5.091	5.091	5.088	5.085	5.062	5.061	5.079	5.080	5.080	5.059	5.062	5.063	5.062
-2	5.000	5.003	4.998	4.999	4.976	4.981	4.999	4.999	5.000	4.981	4.982	4.982	4.985
-3	4.822	4.661	4.662	4.658	4.637	4.373	4.388	4.388	4.393	4.377	4.378	4.383	4.834
E5-1	4.862	4.861	4.857	4.857	4.834	4.837	4.853	4.854		4.835	4.836	4.836	4.833
-2	4.866	4.866	4.864	4.863	4.841	4.841	4.858	4.858		4.840	4.841	4.841	4.839
-3	4.750	4.748	4.742	4.741	4.719	4.717	4.727	4.728		4.708	4.709	4.709	4.706
-4	4.690	4.689	4.677	4.676	4.655	4.644	4.660	4.661		4.640	4.641	4.642	4.639
-5	4.498	4.495	4.486	4.483	4.462	4.453	4.468	4.469		4.444	4.445	4.445	4.443
-6	4.721	4.717	4.708	4.707	4.686	4.676	4.692	4.693		4.668	4.669	4.669	4.667
E6-1	4.837	4.837	4.839		4.811		4.846	4.848		4.829	4.829	4.830	4.829
-2	4.727	4.724	4.721		4.694		4.704	4.705		4.685	4.686	4.688	4.683
-3	4.763	4.759	4.755		4.725		4.734	4.735		4.714	4.715	4.715	4.713
-4	4.689	4.683	4.678		4.648		4.658	4.658		4.634	4.634	4.635	4.633
-5	4.723	4.717	4.717		4.683		4.690	4.690		4.665	4.666	4.661	4.660
-6	4.736	4.730	4.730		4.700		4.712	4.713		4.688	4.689	4.688	4.686
Battery Voltage				10.022	9.977[1]	9.978	10.014[2]			9.975[3]	9.977	9.976	9.977

[1] Fuse replaced

[2] Fuse replaced

[3] Fuse replaced

Voltage Readings (volts)

Instrument I.D.	3-13 16:28	3-13 19:14	3-14 22:27	3-15 08:57	3-15 10:16	3-16 10:13	3-16 14:58	3-19 18:33	3-20 10:07	3-21 08:46	3-26 10:18	3-27 14:30	3-29 14:18	3-29 15:06
E8-1		5.029	5.022	5.012		5.002	4.990	4.986	4.988	4.988	4.991	4.990	4.993	
-2		4.290	4.282	4.246		4.222	4.212	4.210	4.213	4.212	4.211	4.212	4.214	
-3		4.996	4.989	4.900		4.596	4.585	4.551	4.554	4.553	4.563	4.564	4.570	
E9-1		4.936	4.931	4.926		4.925	4.914	4.911	4.909	4.909	4.906	4.907		4.909
-2		4.929	4.924	4.925		4.865	4.854	4.857	4.856	4.856	4.855	4.856		4.860
-3		4.906	4.899	3.448		2.198	2.192	1.930	1.911	1.911	1.908	1.908		1.825
-4		5.009	5.003	4.850		4.739	4.728	4.709	4.710	4.709	4.705	4.705		4.662
-5		4.964	4.969	4.884		4.855	4.844	4.824	4.823	4.822	4.824	4.824		4.792
-6		4.905	4.902	4.871		4.868	4.856	4.843	4.838	4.840	4.838	4.841		4.820
E10-1	4.465		4.464	4.461		4.457	4.447	4.446	4.445	4.444	4.442	4.443		
-2	4.377		4.376	4.354		4.356	4.347	4.340	4.337	4.336	4.335	4.335		
-3	2.447		0.771	0.003	3.316[1]	0.526	0.523	0.000[2]	-----	-----	-----	-----		
-4	4.383		4.399	4.378		4.354	4.344	4.331	4.325	4.325	4.320	4.321		
-5	4.305		4.253	4.120		4.054	4.044	4.031	4.025	4.025	4.020	4.021		
-6	4.543		4.543	4.515		4.486	4.476	4.470	4.465	4.465	4.459	4.459		
Battery Voltage	9.993	9.994	9.994	9.994	-----	-----	9.981[3]	-----	-----	-----	-----	-----	-----	-----

1 Pot rezeroed

2 Pot removed (out of range)

3 Power supply switched from portable readout to L^3 system.

Voltage Readings (volts)

Instrument I.D.	3-29 16:00	3-29 17:00	3-30 10:20	4-2 13:20	4-3 11:30	4-4 01:36	4-4 21:30	4-6 00:26	4-6 06:20	4-10 11:42
E8-1		4.997	5.013	5.010	5.007	5.007	5.005	5.003	5.014	5.000
-2		4.174	4.175	4.176	4.176	4.176	4.189	4.189	4.207	4.209
-3		4.593	4.611	4.609	4.605	4.605	4.618	4.616	4.329	4.321
E9-1	4.923		4.920	4.920	4.920	4.920	4.921	4.921	4.925	4.926
-2	4.876		4.874	4.873	4.873	4.873	4.872	4.871	4.870	4.867
-3	1.837		1.737	1.664	1.521	1.522	1.472	1.472	1.379	1.379
-4	4.683		4.650	4.623	4.556	4.556	4.555	4.554	4.549	4.546
-5	4.817		4.702	4.686	4.690	4.690	4.611	4.611	4.576	4.569
-6	4.846		4.773	4.786	4.782	4.782	4.776	4.776	4.776	4.760
E10-1	4.443	4.446	4.446	4.443	4.444	4.445	4.445	4.445	4.443	4.441
-2	4.333	4.333	4.327	4.324	4.317	4.318	4.312	4.311	4.301	4.299
-3	-----	-----	-----	-----	-----	-----	-----	-----	-----	-----
-4	4.320	4.329	4.325	4.322	4.319	4.320	4.313	4.314	4.300	4.298
-5	4.003	4.010	3.999	3.994	3.984	3.984	3.959	3.959	3.928	3.924
-6	4.459	4.469	4.463	4.458	4.455	4.455	4.450	4.449	4.435	4.433
Battery Voltage	-----	-----	-----	9.981	9.981	9.982	9.981	9.981	9.981	9.979
	(E9)	(E8) (E10)								

Calibration rezeroes

Voltage Readings (volts)

Instrument I.D.	3-15 19:45	3-16 09:13	3-16 15:02	3-19 18:56	31-9 19:10	3-20 09:22	3-21 09:19	3-26 10:46	3-27 14:06	3-29 17:03	3-30 11:03	4-2 13:40	4-3 12:53	4-3 14:10
E11-1	4.995	4.999[1]	5.028	5.023		5.022	5.032	4.969	4.971[5]	5.044	5.029	5.000	5.002	4.999
-2	4.962	4.777	4.804	4.815		4.817	4.819	4.817	4.818	4.814	4.803	4.796	4.796	4.792
-3	5.326	4.832	4.855	4.855		4.855	4.868	4.866	4.866	4.889	4.860	4.831	4.838	4.837
E12-1	4.879	4.875	4.886	9.305[3]	5.036[4]	5.039	5.038	5.036	5.036	5.031	5.025	5.009	-----[6]	-----[6]
-2	4.717	4.532	4.543	4.542		4.541	4.541	4.540	4.540	4.472	4.464	4.451	4.451	4.448
-3	4.799	4.660	4.670	4.672		4.669	4.670	4.667	4.667	4.592	4.582	4.568	4.566	4.563
-4	4.840	4.606	4.617	4.613		4.609	4.609	4.606	4.607	4.358	4.211	4.195	4.193	4.191
-5	4.872	4.716	4.727	4.732		4.731	4.727	4.724	4.724	4.634	4.510	4.496	4.491	4.489
-6	4.915	4.756	4.767	4.768		4.765	4.767	4.765	4.765	4.722	4.655	4.638	4.636	4.634
E13-1	4.953	4.936	4.948	4.951		4.950	4.950	4.947	4.947	4.942	4.935	4.917	4.919	4.916
-2	4.965	4.932	4.944	4.934		4.932	4.931	4.928	4.928	4.901	4.892	4.876	4.876	4.872
-3	4.917	4.859	4.871	4.867		4.866	4.861	4.858	4.858	4.845	4.837	4.822	4.823	4.819
-4	4.959	4.880	4.892	4.886		4.887	4.883	4.881	4.881	4.873	4.866	4.850	4.851	4.847
-5	4.940	4.772	4.785	4.774		4.774	4.768	4.765	4.765	4.759	4.750	4.736	4.737	4.733
-6	4.929	4.869	4.881	4.880		4.878	4.874	4.872	4.872	4.863	4.856	4.841	4.842	4.838
Battery Voltage	9.994	9.991	10.041[2]	-----	-----	-----	-----	-----	-----	-----	-----	9.992[7]	9.994	9.988

1 Extensometer head water filled - dried and read

2 Power supply switched from portable readout to L^3 power supply

3 Pot malfunction?

4 Pot rezeroed

5 Extensometer head water filled - dried and read

6 Erratic behavior

7 Fuse changed

Voltage Readings (volts)

Instrument I.D.	4-4 01:04	4-4 23:27	4-6 03:15	4-6 06:40	4-10 12:14
E11-1	5.003	5.003	5.015[2]	5.003	-----[3]
-2	4.795	4.787	4.792	4.695	-----
-3	4.831	4.829	4.841	4.369	-----
E12-1	5.000[1]	4.999	4.997	4.993	4.994
-2	4.452	4.457	4.457	4.448	4.448
-3	4.567	4.563	4.563	4.548	4.546
-4	4.195	4.182	4.183	4.176	4.175
-5	4.492	4.464	4.464	4.457	4.456
-6	4.638	4.623	4.624	4.604	4.602
E13-1	4.920	4.919	4.922	4.916	4.913
-2	4.878	4.856	4.858	4.813	4.808
-3	4.824	4.801	4.803	4.792	4.789
-4	4.853	4.814	4.816	4.807	4.804
-5	4.739	4.701	4.703	4.694	4.690
-6	4.843	4.811	4.812	4.802	4.799
Battery Voltage	9.993	9.993	9.992	9.992	9.992

1 Pot repaired, tightened, and rezeroed to 5,000 volts

2 Extensometer head water filled, dried out, and read

3 Instrument head damaged due to corrosion of linear pot mounting bracket-readings are meaningless until repaired

APPENDIX B

EXTENSOMETER DISPLACEMENT READINGS

Tables B

Displacement Readings (mm)

Instrument I.D.	3-6 15:30	3-6 17:00	3-7 09:00	3-7 11:30	3-7 15:00	3-8 10:50	3-8 12:00	3-9 07:30	3-9 10:49	3-12 14:50	3-12 18:36	3-13 06:00	3-13 13:51	3-14 22:39
E1-1	0	0	-.003	-.008	-.008	0	0	-.063		-.106	-.116	-.130	-.135	-.137
-2	0	.021	-.007	.181	.175	0	.050	-.145		-.354	-.418	-.248	-.260	-.264
-3	0	.051	.101	.127	.124	0	-.003	-.361		-.964	-1.014	-1.138	-1.398	-1.465
E2-1		0	.001	.004	.004	0	-.001	-.027		-.030	-.039	-.040	-.039	-.043
-2		0	-.001	-.012	-.012	0	.001	-.029		.004	----	-.004	-.011	-.056
-3		0	-.004	.007	.007	0	.001	-.004		.004	.001	-.007	-.003	-.012
-4		0	.007	.020	.020	0	.001	-.423		-.891	-.895	-.902	-.903	-.902
-5		0	.004	.020	.020	0	-.001	.023		-.080	-.076	-.099	-.100	-.085
-6		0	-.015	-.042	-.042	0	.001	.007		-.088	-.106	-.121	-.119	-.107
E3-1		0	-.004	-.009	-.007				0	.005	-.007	0	-.001	-.005
-2		0	.004	.009	.009				0	-.043	-.057	-.051	-.047	-.053
-3		0	-.001	.021	.021				0	-.086	-.096	-.103	-.102	-.109
-4		0	-.001	.012	.010				0	-.098	-.111	-.115	-.119	-.123
-5		0	-.004	.015	.015				0	-.011	-.025	-.024	-.031	-.045
-6		0	.009	.030	.035				0	.049	.032	.029	.035	.031
	2+32	2+38	2+44	2+50		2+55 2+63		2+68 2+76		2+83 2+89	2+96	3+02	3+11	3+19

Displacement Readings (mm)

Instrument I.D.	3-15 08:45	3-16 10:01	3-16 15:37	3-20 09:51	3-21 08:48	3-22 19:42	3-22 20:25	3-23	3-23 12:38	3-23 13:15	3-23 ~14:00	3-26 10:05	3-27 14:18	3-29 13:13
E1-1	-.135	-.135	-.149	-.149	-.149	-.149	-.149					-.151	-.149	-.149
-2	-.261	-.260	-.273	-.270	-.270	-.270	-.270					-.273	-.267	-.246
-3	-1.476	-1.474	-1.488	-1.480	-1.478	-1.480	-1.479					-1.490	-1.487	-1.515
E2-1	-.040	-.039	-.054	-.054	-.054	-.056	-.059	-.059	-.069			-.074	-.074	-.064
-2	-.004	-.003	-.017	-.015	-.015	-.017	-.017	-.017	-.031			-.039	-.037	-.015
-3	-.001	.004	-.007	-.004	-.004	-.010	-.010	-.009	.004			-.001	.001	.010
-4	-.888	-.882	-.893	-.888	-.888	-.893	-.890	-.899	-.904			-.913	-.910	-.902
-5	-.061	-.060	-.072	-.061	-.061	-.064	-.064	-.065	-.054			-.059	-.051	-.035
-6	-.086	-.084	-.097	-.091	-.091	-.091	-.094	-.094	-.118			-.126	-.121	-.216
E3-1	-.003	-.004	-.016	-.019	-.019	-.022				-.030	-.029	-.032	-.032	-.040
-2	-.048	-.047	-.062	-.067	-.067	-.069				-.085	-.085	-.093	-.091	-.115
-3	-.106	-.104	-.120	-.117	-.117	-.123				-.131	-.131	-.137	-.134	-.204
-4	-.123	-.124	-.137	-.139	-.139	-.142				-.153	-.153	-.161	-.158	-.199
-5	-.048	-.044	-.059	-.059	-.059	-.061				-.064	-.064	-.069	-.066	-.184
-6	.036	.035	.023	.023	.023	.020				.018	.018	.013	.013	-.083
	3+27 3+35	3+42 3+49		3+57 3+62 3+70 3+77 3+86	3+95 3+95 End Top Heading	2+05			2+33					2+59 2+72

Displacement Readings (mm)

Instrument I.D.	3-30 10:30	4-2 12:17	4-3 11:40	4-4 01:26	4-4 21:21	4-6 00:16	4-6 06:11	4-10 11:27
E1-1	-.143	-.149	-.134	-.132	-.130	-.130	-.131	-.138
-2	-.238	-.241	-.171	-.172	-.156	-.156	-.152	-.154
-3	-1.505	-1.510	-1.427	-1.428	-1.400	-1.402	-1.416	-1.420
E2-1	-.064	-.069	-.073	-.074	-.077	-.074	-.073	-.079
-2	-.017	-.023	-.032	-.034	-.037	-.037	-.041	-.045
-3	.010	.004	-.041	-.042	-.040	-.042	-.035	-.040
-4	-.899	-.902	-.949	-.948	-.945	-.948	-.938	-.948
-5	-.027	-.029	-.085	-.087	-.073	-.076	-.069	-.070
-6	-.211	-.216	-.258	-.260	-.260	-.260	-.264	-.270
E3-1	-.040	-.045	-.039	-.037	-.035	-.035	-.036	-.040
-2	-.115	-.120	-.140	-.139	-.136	-.136	-.137	-.141
-3	-.207	-.209	-.241	-.240	-.232	-.232	-.227	-.234
-4	-.197	-.208	-.250	-.249	-.246	-.249	-.242	-.243
-5	-.184	-.184	-.225	-.227	-.213	-.213	-.223	-.224
-6	-.086	-.089	-.113	-.112	-.115	-.112	-.113	-.117
			3+00		3+24		3+60	3+94

Displacement Readings (mm)

Instrument I.D.	3-6 14:30	3-6 17:40	3-7 08:40	3-7 10:30	3-7 11:30	3-7 13:40	3-7 14:45	3-8 09:00	3-8 13:00	3-8 15:00	3-9 08:00	3-12 15:15	3-12 18:22	3-13 05:23
E4-1	0	-.003	.005	.005	-.005			-.011	-.011	-.013	-.055	-.145	-.239	-.263
-2	0	.003	.003	.003	-.016			-.011	-.011	-.011	-.045	-.118	-.205	-.221
-3	0	-.022	-.025	-.025	-.022			-.022	-.025	-.025	-.424	-.787	-.857	-.875
E5-1	0	.005	.003			.003		-.003	0	0	-.013	-.023	-.036	-.039
-2	0	.008	.005			.005		-.010	-.010	-.008	-.033	-.003	-.008	-.013
-3	0	.008	.008			.008		0	-.003	0	-.178	-.200	-.228	-.239
-4	0	-.003	-.005			-.005		-.021	-.021	-.021	-.187	-.274	-.330	-.349
-5	0	-.033	-.033			-.033		-.053	-.055	-.055	-.293	-.593	-.625	-.643
-6	0	-.029	-.029			-.029		-.066	-.066	-.066	-.280	-.509	-.538	-.569
E6-1	0	.003	0		.003		.003	.003	-.003	0	-.014	-.022	-.035	-.046
-2	0	.005	.010		.008		.008	-.029	-.031	-.029	-.070	-.197	-.226	-.234
-3	0	.003	0		.003		.003	-.013	-.013	-.016	-.054	-.147	-.178	-.204
-4	0	.003	.011		.014		.014	-.038	-.041	-.041	-.084	-.261	-.245	-.269
-5	0	0	-.003		-.003		-.003	-.055	-.057	-.057	-.156	-.259	-.278	-.322
-6	0	0	.009		.018		.018	-.015	-.015	-.015	-.076	-.202	-.221	-.232
	2+32	2+38	2+44		2+50			2+55 2+63			2+68 2+76	2+83 2+89	2+96	3+02

Displacement Readings (mm)

Instrument I.D.	3-13 14:22	3-14 22:48	3-15 08:31	3-16 09:48	3-16 15:18	3-20 09:29	3-21 09:11	3-22 13:15	3-22 13:20	3-22 14:14	3-22 18:11	3-22 18:50	3-22 20:00	3-26 10:32
E4-1	-.292	-.297	-.303	-.310	-.329	-.324	-.324	-.326		-.329	-.329			-.334
-2	-.258	-.258	-.255	-.260	-.276	-.274	-.274	-.276		-.278	-.278			-.288
-3	-.896	-.893	-.833	-.891	-.909	-.893	-.893	-.893		-.894	-.894			-.902
E5-1	-.034	-.039	-.039	-.042	-.057	-.057	-.054		-.058			-.058		-.071
-2	-.020	-.023	-.020	-.026	-.038	-.036	-.033		-.037			-.037		-.050
-3	-.245	-.248	-.248	-.253	-.267	-.264	-.261		-.270			-.270		-.286
-4	-.360	-.360	-.357	-.362	-.376	-.370	-.368		-.373			-.373		-.378
-5	-.648	-.651	-.643	-.648	-.663	-.658	-.658		-.664			-.664		-.659
-6	-.569	-.569	-.563	-.566	-.580	-.578	-.578		-.583			-.583		-.572
E6-1	-.049	-.052	-.049	-.055	-.068	-.065	-.068	-.068					-.070	-.083
-2	-.239	-.241	-.241	-.244	-.231	-.262	-.262	-.262					-.263	-.258
-3	-.209	-.217	-.217	-.222	-.235	-.233	-.235	-.235					-.235	-.246
-4	-.283	-.291	-.296	-.294	-.307	-.304	-.307	-.307					-.307	-.304
-5	-.333	-.336	-.360	-.363	-.377	-.374	-.377	-.377					-.378	-.334
-6	-.249	-.257	-.263	-.263	-.279	-.276	-.276	-.279					-.280	-.280
	3+11	3+19	3+27 3+35	3+42 3+49		3+57 3+62 3+70 3+77 3+86	3+95 End Top Heading	2+05						2+33

Displacement Readings (mm)

Instrument I.D.	3-27 14:00	3-29 13:26	3-30 10:44	4-2 12:49	4-2 13:00	4-3 11:52	4-3 12:10	4-4 01:15	4-4 22:22	4-4 22:32	4-6 00:38	4-6 06:31	4-10 12:04
E4-1	-.331	-.331	-.339	-.347	-.337	-.340	-.342	-.339	-.339	-.342	-.334	-.332	-.334
-2	-.283	-.275	-.288	-.275	-.276	-.263	-.264	-.264	-.262	-.262	-.259	-.259	-.251
-3	-.894	-1.310	-1.308	-1.318	-1.309	-1.994	-1.997	-1.997	-1.984	-1.983	-1.980	-1.967	-1.964
E5-1	-.069	-.071	-.082	-.072	-.075	-.067	-.072	-.069		-.070	-.067	-.067	-.075
-2	-.045	-.045	-.050	-.052	-.043	-.043	-.045	-.045		-.044	-.042	-.042	-.047
-3	-.284	-.289	-.306	-.309	-.297	-.303	-.275	-.272		-.328	-.325	-.325	-.334
-4	-.375	-.378	-.410	-.403	-.403	-.432	-.435	-.432		-.441	-.439	-.436	-.444
-5	-.656	-.564	-.686	-.694	-.687	-.710	-.714	-.711		-.730	-.728	-.728	-.728
-6	-.569	-.580	-.606	-.609	-.596	-.625	-.630	-.627		-.548	-.645	-.645	-.651
E6-1	-.078	-.078	-.072		-.079		-.032	-.027		-.028	-.028	-.026	-.028
-2	-.253	-.261	-.269		-.274		-.293	-.290		-.296	-.293	-.288	-.301
-3	-.243	-.253	-.264		-.276		-.298	-.296		-.303	-.301	-.301	-.306
-4	-.299	-.315	-.329		-.343		-.363	-.363		-.380	-.380	-.377	-.383
-5	-.332	-.348	-.348		-.373		-.401	-.401		-.421	-.418	-.432	-.434
-6	-.275	-.291	-.291		-.305		-.320	-.317		-.337	-.334	-.337	-.342
		2+59 2+72				3+00			3+24			3+60	3+94

Displacement Readings (mm)

Instrument I.D.	3-13 16:28	3-13 19:14	3-14 22:27	3-15 08:57	3-15 10:16	3-16 10:13	3-16 14:58	3-19 18:33	3-20 10:07	3-21 08:46	3-26 10:18	3-27 14:30	3-29 14:18	3-29 15:06
E8-1		0	-.019	-.047		-.074	-.089	-.100	-.095	-.095	-.086	-.089	-.081	
-2		0	-.021	-.117		-.181	-.193	-.199	-.191	-.193	-.196	-.193	-.188	
-3		0	-.018	-.250		-1.040	-1.053	-1.142	-1.134	-1.137	-1.111	-1.108	-1.093	
E9-1		0	-.013	-.026		-.029	-.041	-.049	-.054	-.054	-.062	-.059		-.054
-2		0	-.013	-.011		-.172	-.185	-.177	-.180	-.180	-.182	-.180		-.169
-3		0	-.019	-3.901		-7.245	-7.254	-7.956	-8.006	-8.006	-8.015	-8.015		-8.237
-4		0	-.017	-.457		-.776	-.790	-.845	-.842	-.845	-.857	-.857		-.980
-5		0	.014	-.230		-.313	-.327	-.385	-.387	-.390	-.385	-.385		-.477
-6		0	-.008	-.089		-.096	-.111	-.145	-.158	-.153	-.158	-.150		-.205
E10-1	0		-.003	-.011		-.021	-.032	-.035	-.037	-.040	-.045	-.043		
-2	0		-.003	-.062		-.057	-.066	-.085	-.093	-.095	-.098	-.098		
-3	0		-4.453	-6.494	-6.494	-13.907	-13.915	>-15.3	-----	-----	-----	-----		
-4	0		.044	-.014		-.080	-.092	-.128	-.144	-.144	-.158	-.155		
-5	0		-.143	-.510		-.692	-.705	-.741	-.758	-.758	-.772	-.769		
-6	0		0	-.077		-.157	-.169	-.185	-.199	-.199	-.216	-.216		
	3+11		3+19	3+27 3+35		3+42 3+49		3+57 3+62 3+77	3+86	3+95 3+95 End Top Heading 2+05	2+33		2+59 2+72	

Displacement Readings (mm)

Instrument I.D.	3-29 16:00	3-29 17:00	3-30 10:20	4-2 13:20	4-3 11:30	4-4 01:36	4-4 21:30	4-6 00:26	4-6 06:20	4-10 11:42
E8-1		-.081	-.037	-.045	-.053	-.053	-.059	-.064	-.034	-.073
-2		-.188	-.185	-.183	-.183	-.183	-.148	-.148	-.100	-.094
-3		-1.093	-1.046	-1.051	-1.061	-1.061	-1.027	-1.033	-1.780	-1.801
E9-1	-.054		-.062	-.062	-.062	-.062	-.059	-.059	-.049	-.046
-2	-.169		-.174	-.177	-.177	-.177	-.180	-.182	-.185	-.193
-3	-8.237		-8.505	-8.700	-9.083	-9.081	-9.215	-9.215	-9.464	-9.464
-4	-.980		-1.075	-1.153	-1.346	-1.346	-1.349	-1.352	-1.366	-1.375
-5	-.477		-.808	-.854	-.842	-.842	-1.070	-1.070	-1.171	-1.191
-6	-.205		-.396	-.362	-.372	-.372	-.388	-.388	-.414	-.430
E10-1	-.043	-.043	-.043	-.051	-.048	-.045	-.045	-.045	-.051	-.056
-2	-.098	-.098	-.114	-.122	-.141	-.139	-.155	-.158	-.185	-.190
-3	-----	-----	-----	-----	-----	-----	-----	-----	-----	-----
-4	-.155	-.158	-.169	-.178	-.186	-.183	-.202	-.200	-.238	-.244
-5	-.819	-.799	-.830	-.844	-.871	-.871	-.940	-.940	-1.026	-1.037
-6	-.216	-.216	-.232	-.246	-.254	-.254	-.268	-.271	-.310	-.315
					3+00		3+24		3+60	3+94

Displacement Readings (mm)

Instrument I.D.	3-15 19:45	3-16 09:13	3-16 15:02	3-19 18:56	3-19 19:10	3-20 09:22	3-21 09:19	3-26 10·46	3-27 14:06	3-29 17:03	3-30 11:03	4-2 13:40	4-3 12:53	4-3 14:10
E11-1	0	.010	.025	.012		.009	.035	-.128	-.123	.066	.027	.014	.019	.012
-2	0	-.515	-.502	-.472		-.466	-.461	-.466	-.463	-.474	-.505	-.460	-.460	-.472
-3	0	-1.372	-1.372	-1.371		-1.371	-1.335	-1.341	-1.341	-1.277	-1.357	-1.373	-1.354	-1.357
E12-1	0	-.011	-.043	11.815?	0	0.008	0.005	0	0	-.013	-.030	-.072	-----	-----
-2	0	-.499	-.526	-.529		-.532	-.532	-.534	-.534	-.717	-.738	-.716	-.716	-.724
-3	0	-.381	-.414	-.408		-.416	-.414	-.422	-.422	-.627	-.654	-.632	-.638	-.646
-4	0	-.647	-.676	-.687		-.698	-.698	-.706	-.703	-1.388	-1.792	-1.781	-1.787	-1.792
-5	0	-.435	-.466	-.452		-.455	-.466	-.474	-.474	-.723	-1.067	-1.046	-1.060	-1.066
-6	0	-.460	-.493	-.490		-.499	-.493	-.499	-.499	-.623	-.815	-.800	-.806	-.812
E13-1	0	-.045	-.074	-.066		-.069	-.069	-.076	-.076	-.089	-.108	-.093	-.088	-.096
-2	0	-.091	-.122	-.150		-.155	-.158	-.166	-.166	-.240	-.265	-.245	-.245	-.256
-3	0	-.154	-.182	-.193		-.196	-.209	-.217	-.217	-.251	-.272	-.251	-.248	-.259
-4	0	-.213	-.242	-.258		-.256	-.266	-.272	-.272	-.293	-.312	-.292	-.290	-.300
-5	0	-.435	-.459	-.487		-.487	-.503	-.510	-.510	-.526	-.549	-.527	-.524	-.534
-6	0	-.155	-.183	-.186		-.191	-.201	-.206	-.206	-.230	-.248	-.226	-.224	-.234
	3+35	3+42 3+49		3+57 3+62 3+70		3+77 3+86	3+95 3+95 End Top Heading 2+05	2+33		2+59 2+72			3+00	

Displacement Readings (mm)

Instrument I.D.	4-4 01:04	4-4 23:27	4-6 03:15	4-6 06:40	4-10 12:14
E11-1	.022	.022	.053	.022	-----
-2	-.463	-.486	-.472	-.741	-----
-3	-1.373	-1.379	-1.345	-2.656	-----
E12-1	0	-.003	-.008	-.019	-.016
-2	-.713	-.700	-.70[illegible]	-.724	-.724
-3	-.635	-.646	-.64[illegible]	-.687	-.692
-4	-1.781	-1.817	-1.814	-1.833	-1.836
-5	-1.057	-1.135	-1.135	-1.155	-1.158
-6	-.800	-.844	-.841	-.899	-.904
E13-1	-.085	-.088	-.080	-.096	-.104
-2	-.239	-.300	-.295	-.419	-.433
-3	-.245	-.306	-.301	-.330	-.338
-4	-.284	-.389	-.384	-.408	-.416
-5	-.519	-.617	-.612	-.635	-.646
-6	-.221	-.304	-.301	-.327	-.335
		3+24		3+60	3+94

APPENDIX C

EXTENSOMETER MINE-BY CALIBRATION DATA

Tables C-1

Mine-By - Calibration Data

	10.0 mm	11.0 mm	12.0 mm	13.0 mm	14.0 mm	15.0 mm	12.0 mm
E1-1	3.834	4.225	4.589	4.956	5.341	5.743	
	10.000	11.032	11.992	12.961	13.977	15.038	
	3.819	4.201	4.560	4.924	5.332	5.717	4.554
	10.015	11.026	11.976	12.940	14.020	15.023	11.960
E1-2	3.831	4.172	4.582	4.952	5.338	5.731	
	10.049	10.941	12.014	12.982	13.993	15.021	
	3.739	4.128	4.482	4.867	5.240	5.626	4.478
	9.996	11.031	11.972	12.997	13.989	15.016	11.962
E1-3	3.814	4.174	4.553	4.948	5.347	5.751	
	10.055	10.981	11.956	12.972	13.999	15.038	
	4.132	4.513	4.913	5.296	5.726	6.079	4.911
	10.013	10.982	11.999	12.973	14.067	14.965	11.994

Mine-By Calibration Data

	10 mm	11 mm	12 mm	13 mm	14 mm	15 mm	12 mm	13 mm
E2-1	4.192	4.579	4.978	5.360	5.751	6.115		
	9.987	10.989	12.022	13.011	14.024	14.967		
	4.194	4.579	4.968	5.354	5.743	6.101	4.968	5.352
	9.989	10.993	12.008	13.015	14.030	14.964	12.008	13.010
E2-2	4.315	4.684	5.064	5.428	5.790	6.142		
	9.982	10.990	12.027	13.021	14.009	14.971		
	4.315	4.665	5.057	5.423	5.781	6.119	5.048	5.423
	9.995	10.957	12.034	13.039	14.023	14.952	12.009	13.039
E2-3	4.286	4.648	5.005	5.364	5.750	6.129		
	10.025	11.009	11.978	12.954	14.002	15.032		
	4.298	4.642	5.004	5.368	5.756	6.109	4.989	5.368
	10.037	10.980	11.973	12.971	14.035	15.003	11.932	12.971
E2-4	4.247	4.635	5.000	5.368	5.747	6.098		
	9.974	11.022	12.007	13.001	14.024	14.972		
	3.952	4.302	4.683	5.043	5.426	5.791	4.680	5.041
	10.025	10.973	12.004	12.979	14.016	15.004	11.996	12.973
E2-5	4.301	4.676	5.046	5.421	5.799	6.150		
	9.991	11.002	11.998	13.009	14.027	14.973		
	4.298	4.665	5.039	5.409	5.779	6.118	5.024	5.411
	9.987	10.990	12.011	13.022	14.032	14.958	11.970	13.027
E2-6	4.288	4.647	5.018	5.379	5.767	6.123		
	10.015	10.989	11.996	12.976	14.029	14.995		
	4.269	4.585	4.936	5.366	5.723	6.003	4.997	5.368
	10.052	10.993	11.912	13.111	14.106	14.887	12.082	13.116

I

Mine-By Calibration Data

	10 mm	11 mm	12 mm	13 mm	14 mm	15 mm	12 mm
E3-1	4.235	4.582	4.958	5.334	5.724	6.107	
	10.050	10.972	11.972	12.971	14.008	15.026	
	4.221	4.572	4.951	5.316	5.705	6.097	4.953
	10.044	10.978	11.987	12.959	13.994	15.038	11.992
E3-2	4.225	4.595	4.965	5.331	5.707	6.072	
	10.000	11.001	12.002	12.992	14.009	14.997	
	4.197	4.569	4.942	5.299	5.677	6.050	4.938
	9.998	11.004	12.012	12.978	13.999	15.008	12.002
E3-3	4.244	4.583	4.971	5.325	5.677	6.011	
	10.000	10.951	12.039	13.033	14.020	14.957	
	4.175	4.535	4.906	5.264	5.631	5.982	4.929
	9.996	10.990	12.014	13.002	14.015	14.983	12.077
E3-4	4.287	4.633	5.005	5.373	5.749	6.115	
	10.032	10.974	11.986	12.988	14.012	15.008	
	4.242	4.588	4.958	5.320	5.698	6.063	4.963
	10.031	10.977	11.989	12.979	14.013	15.011	12.003
E3-5	4.294	4.616	5.025	5.411	5.778	6.114	
	10.041	10.909	12.011	13.052	14.041	14.947	
	4.222	4.577	4.958	5.329	5.716	6.094	5.008
	10.032	10.997	11.991	12.978	14.008	15.014	12.124
E3-6	4.119	4.542	4.968	5.350	5.723	6.078	
	9.925	11.002	12.087	13.060	14.011	14.915	
	4.132	4.496	4.895	5.249	5.661	6.058	4.966
	10.035	10.979	12.015	12.934	14.003	15.034	12.199

Mine-By Calibration Data

	10 mm	11 mm	12 mm	13 mm	14 mm	15 mm	14 mm	12 mm
E4-1	4.343	4.708	5.070	5.451	5.847	6.257		
	10.050	11.005	11.952	12.949	13.985	15.058		
	4.362	4.733	5.093	5.472	5.868	6.251		5.094
	10.028	11.010	11.962	12.964	14.012	15.025		11.965
	4.366	4.729	5.089	5.474	5.869	6.250	5.868	5.090
	10.039	10.999	11.952	12.970	14.016	15.024	14.013	11.955
E4-2	4.247	4.622	4.995	5.354	5.758	6.156		
	10.025	11.011	11.991	12.935	13.996	15.042		
	4.245	4.626	5.005	5.350	5.735	6.124		5.003
	9.994	11.014	12.029	12.953	13.984	15.026		12.024
	4.252	4.620	5.003	5.357	5.748	6.138	5.747	5.002
	10.017	10.995	12.013	12.954	13.993	15.029	13.990	12.010
E4-3	4.312	4.669	5.069	5.457	5.846	6.257		
	10.048	10.963	11.989	12.984	13.981	15.035		
	4.090	4.449	4.820	5.212	5.618	5.996		4.821
	10.049	10.984	11.951	12.972	14.030	15.015		11.953
	4.092	4.446	4.818	5.209	5.617	5.993	5.617	4.818
	10.055	10.979	11.949	12.969	14.034	15.015	14.034	11.949

Mine-By Calibration Data

	10 mm	11 mm	12 mm	13 mm	14 mm	15 mm	12 mm
E5-1	4.107	4.477	4.839	5.229	5.639	6.027	
	10.044	11.005	11.944	12.957	14.021	15.028	
	4.126	4.483	4.858	5.241	5.655	6.043	4.862
	10.057	10.983	11.956	12.950	14.024	15.030	11.966
E5-2	4.052	4.458	4.838	5.248	5.631	6.005	
	9.979	11.016	11.987	13.035	14.014	14.969	
	4.079	4.474	4.863	5.274	5.654	6.032	4.862
	9.990	10.998	11.991	13.039	14.009	14.973	11.988
E5-3	4.086	4.455	4.813	5.164	5.529	5.886	
	9.987	11.014	12.011	12.988	14.004	14.997	
	4.032	4.390	4.750	5.108	5.470	5.832	4.751
	10.004	10.999	11.999	12.994	13.999	15.005	12.002
E5-4	4.034	4.408	4.784	5.167	5.541	5.903	
	9.997	10.994	11.997	13.018	14.015	14.980	
	3.939	4.313	4.690	5.071	5.449	5.810	4.689
	9.998	10.994	11.998	13.012	14.019	14.980	11.995
E5-5	3.919	4.320	4.697	5.102	5.522	5.898	
	10.007	11.016	11.965	12.984	14.041	14.987	
	3.733	4.115	4.494	4.895	5.304	5.708	4.493
	10.035	11.001	11.959	12.972	14.006	15.027	11.956
E5-6	4.166	4.533	4.872	5.216	5.563	5.916	
	9.977	11.031	12.005	12.993	13.990	15.004	
	3.992	4.374	4.713	5.058	5.414	5.757	4.712
	9.958	11.046	12.011	12.994	14.007	14.984	12.008

Mine-By Calibration Data

	10 mm	11 mm	12 mm	13 mm	14 mm	15 mm	12 mm
E6-1	4.138	4.496	4.898	5.175	5.555	5.924	
	9.980	10.990	12.125	12.906	13.979	15.020	
		4.511	4.895	5.196	5.672	6.013	4.840
		11.033	12.045	12.838	14.092	14.991	11.900
E6-2	4.001	4.414	4.785	5.155	5.549	5.935	
	9.970	11.045	12.010	12.973	13.999	15.003	
		4.352	4.718	5.110	5.509	5.888	4.722
		11.024	11.971	12.986	14.019	15.000	11.982
E6-3	4.050	4.427	4.814	5.191	5.589	5.972	
	10.014	10.993	11.998	12.978	14.011	15.006	
		4.382	4.763	5.147	5.547	5.934	4.763
		11.013	11.993	12.980	14.009	15.004	11.993
E6-4	4.031	4.391	4.757	5.097	5.480	5.863	
	10.018	11.005	12.008	12.940	13.989	15.039	
		4.332	4.682	5.053	5.432	5.811	4.685
		11.032	11.975	12.976	13.998	15.019	11.984
E6-5	4.045	4.407	4.777	5.135	5.517	5.872	
	10.006	10.994	12.004	12.981	14.023	14.992	
		4.357	4.699	5.096	5.509	5.834	4.701
		11.032	11.939	12.992	14.088	14.950	11.944
E6-6	4.077	4.442	4.799	5.156	5.524	5.884	
	9.998	11.009	11.998	12.986	14.006	15.003	
		4.380	4.731	5.098	5.483	5.838	4.733
		11.021	11.978	12.978	14.028	14.995	11.983

Mine-By Calibration Data

	10 mm	11 mm	12 mm	13 mm	14 mm	15 mm	12 mm
E8-1	4.263	4.563	5.010	5.372	5.748	6.094	
	10.062	10.864	12.059	13.027	14.032	14.956	
	4.252	4.622	4.997	5.360	5.724	6.074	4.997
	9.982	10.995	12.022	13.016	14.013	14.972	12.022
E8-2	3.469	3.845	4.222	4.583	4.979	5.355	
	10.007	11.004	12.004	12.962	14.012	15.010	
	3.435	3.802	4.179	4.543	4.927	5.303	4.175
	10.012	10.994	12.003	12.977	14.004	15.010	11.992
E8-3	4.183	4.631	4.950	5.332	5.752	6.109	
	9.948	11.119	11.953	12.951	14.048	14.981	
	3.842	4.224	4.598	4.985	5.376	5.765	4.594
	10.013	11.006	11.979	12.985	14.002	15.014	11.969

Mine-By Calibration Data

	10 mm	11 mm	12 mm	13 mm	14 mm	15 mm	12 mm
E9-1	4.150	4.532	4.926	5.308	5.690	6.059	
	9.991	10.988	12.017	13.015	14.013	14.976	
	-----	4.529	4.922	5.302	5.683	6.054	4.922
		10.982	12.013	13.010	14.010	14.984	12.013
E9-2	4.173	4.559	4.911	5.276	5.663	6.035	
	9.995	11.035	11.983	12.967	14.009	15.012	
	-----	4.505	4.876	5.239	5.621	5.988	4.876
		11.004	12.004	12.982	14.011	15.000	12.004
E9-3	4.143	4.509	4.887	5.279	5.667	6.018	
	10.014	10.981	11.980	13.016	14.041	14.969	
	-----	1.459	1.842	2.218	2.584	2.934	1.838
		10.974	12.011	13.029	14.020	14.967	12.000
E9-4	4.313	4.658	4.983	5.330	5.691	6.061	
	10.032	11.023	11.956	12.952	13.988	15.050	
	-----	4.344	4.683	5.026	5.377	5.733	4.683
		11.017	11.993	12.981	13.992	15.017	11.993
E9-5	4.220	4.578	4.947	5.298	5.682	6.058	
	10.021	10.996	12.000	12.956	14.002	15.025	
	-----	4.424	4.810	5.174	5.550	5.934	4.817
		10.994	12.020	12.988	13.988	15.009	12.039
E9-6	4.150	4.538	4.896	5.265	5.668	6.047	
	10.006	11.031	11.977	12.952	14.017	15.018	
	-----	4.440	4.837	5.219	5.602	6.002	4.845
		10.994	12.015	12.997	13.982	15.011	12.036

Mine-By Calibration Data

	10 mm	11 mm	12 mm	13 mm	14 mm	15 mm	12 mm
E10-1	3.682	4.069	4.454	4.824	5.213	5.587	
	9.989	11.005	12.016	12.988	14.010	14.992	
	3.674	4.059	4.443	4.815	5.202	5.573	4.444
	9.990	11.003	12.014	12.993	14.012	14.988	12.017
E10-2	3.634	4.007	4.368	4.731	5.119	5.483	
	10.004	11.013	11.989	12.970	14.019	15.004	
	3.583	3.971	4.329	4.695	5.079	5.444	4.330
	9.985	11.030	11.994	12.980	14.014	14.997	11.997
E10-3	1.684	2.056	2.444	2.808	3.191	3.565	
	10.001	10.989	12.020	12.987	14.005	14.998	
	-----	-----	-----	-----	-----	-----	-----
E10-4	3.679	4.006	4.388	4.753	5.099	5.482	
	10.043	10.947	12.003	13.012	13.968	15.027	
	3.600	3.967	4.329	4.679	5.051	5.425	4.328
	10.002	11.011	12.006	12.969	13.992	15.020	12.004
E10-5	3.562	3.921	4.296	4.676	5.063	5.480	
	10.052	10.989	11.968	12.960	13.971	15.060	
	3.267	3.643	4.001	4.369	4.768	5.158	4.010
	10.024	11.021	11.970	12.945	14.003	15.037	11.994
E10-6	3.816	4.165	4.537	4.898	5.259	5.616	
	10.011	10.977	12.007	13.006	14.005	14.994	
	3.734	4.110	4.470	4.816	5.206	5.553	4.469
	9.987	11.021	12.010	12.961	14.034	14.987	12.007

Mine-By Calibration Data

	10 mm	11 mm	12 mm	13 mm	14 mm	15 mm
E11-1	4.220	4.609	4.989	5.355	5.769	6.149
	10.005	11.014	12.000	12.949	14.023	15.009
-2	4.246	4.610	4.949	5.308	5.710	6.029
	10.007	11.020	11.963	12.962	14.080	14.967
-3	4.586	4.951	5.316	5.667	6.045	6.380
	9.988	11.001	12.015	12.989	14.039	14.969
E12-1	4.110	4.492	4.860	5.220	5.596	5.972
	9.988	11.018	12.010	12.981	13.994	15.008
-2	3.974	4.345	4.702	5.066	5.444	5.816
	10.006	11.015	11.986	12.975	14.003	15.015
-3	4.078	4.462	4.793	5.157	5.558	5.899
	9.996	11.049	11.957	12.955	14.054	14.989
-4	4.124	4.446	4.789	5.158	5.576	5.902
	10.082	10.972	11.919	12.939	14.094	14.994
-5	4.157	4.488	4.822	5.180	5.597	5.929
	10.071	10.993	11.924	12.921	14.083	15.008
-6	4.192	4.566	4.932	5.267	5.603	5.919
	9.930	11.013	12.072	13.042	14.014	14.929

Mine-By Calibration Data

	10 mm	11 mm	12 mm	13 mm	14 mm	15 mm
E13-1	4.165	4.539	4.925	5.304	5.696	6.066
	10.008	10.988	12.000	12.993	14.020	14.990
-2	4.203	4.591	4.955	5.307	5.670	6.016
	9.954	11.027	12.034	13.007	14.011	14.967
-3	4.155	4.541	4.913	5.297	5.677	6.037
	9.986	11.009	11.995	13.013	14.021	14.975
-4	4.196	4.582	4.941	5.322	5.696	6.049
	9.981	11.021	11.988	13.015	14.022	14.973
-5	4.147	4.534	4.909	5.303	5.702	6.073
	10.005	11.006	11.977	12.996	14.028	14.988
-6	4.163	4.530	4.897	5.260	5.622	5.950
	9.975	10.996	12.018	13.028	14.035	14.948

Tables C-2

Calibration Statistics

Instrument I.D.	Least Squares Slope (mm/volt)	Correlation Coefficient (r^2)	Sample Variance Sy (mm)
E1-1	2.639	0.9997	0.028
	2.647	0.9997	0.032
-2	2.617	0.9996	0.034
	2.660	0.9999	0.019
-3	2.572	0.9996	0.035
	2.543	0.9996	0.034
E2-1	2.590	0.9999	0.021
	2.609	0.9998	0.021
-2	2.730	0.9999	0.021
	2.747	0.9996	0.035
-3	2.717	0.9998	0.027
	2.742	0.9997	0.027
-4	2.700	0.9999	0.021
	2.707	0.9999	0.019
-5	2.694	0.9999	0.016
	2.731	0.9998	0.025
-6	2.714	0.9999	0.017
	2.739	0.9971	0.092
E3-1	2.658	0.9997	0.031
	2.662	0.9997	0.031
-2	2.705	1.0000	0.005
	2.703	1.0000	0.011
-3	2.805	0.9996	0.035
	2.760	1.0000	0.011
-4	2.722	0.9999	0.019
	2.735	0.9999	0.020
-5	2.695	0.9990	0.054
	2.662	0.9994	0.020
-6	2.547	0.9986	0.064
	2.596	0.9996	0.035
E4-1	2.617	0.9994	0.043
	2.645	0.9998	0.027
	2.646	0.9997	0.030
-2	2.628	0.9996	0.034
	2.678	0.9998	0.026
	2.657	0.9998	0.024
-3	2.564	0.9997	0.031
	2.605	0.9996	0.034
	2.605	0.9996	0.037
E5-1	2.596	0.9995	0.037
	2.594	0.9995	0.040
-2	2.555	0.9998	0.023
	2.551	0.9999	0.021
-3	2.784	1.0000	0.010
	2.778	1.0000	0.004
-4	2.666	0.9999	0.013
	2.663	0.9999	0.012

Instrument I.D.	Least Squares Slope (mm/volt)	Correlation Coefficient (r^2)	Samples Variance Sy (mm)
E5-5	2.516	0.9998	0.025
	2.528	0.9997	0.027
-6	2.872	0.9999	0.017
	2.847	0.9998	0.027
E6-1	2.822	0.9985	0.065
	2.635	0.9962	0.087
-2	2.603	0.9998	0.025
	2.588	0.9998	0.020
-3	2.598	0.9999	0.012
	2.572	0.9999	0.012
-4	2.741	0.9997	0.031
	2.696	0.9997	0.023
-5	2.729	0.9999	0.013
	2.653	0.9985	0.055
-6	2.769	1.0000	0.007
	2.726	0.9998	0.021
E8-1	2.673	0.9983	0.070
	2.739	0.9999	0.019
-2	2.653	0.9999	0.017
	2.676	1.0000	0.012
-3	2.613	0.9986	0.063
	2.601	0.9999	0.013
E9-1	2.612	0.9999	0.016
	2.624	0.9999	0.014
-2	2.695	0.9998	0.022
	2.695	1.0000	0.010
-3	2.643	0.9998	0.025
	2.708	0.9997	0.025
-4	2.871	0.9995	0.038
	2.880	0.9999	0.015
-5	2.723	0.9998	0.022
	2.659	0.9999	0.013
-6	2.642	0.9997	0.027
	2.571	0.9999	0.012
E10-1	2.626	1.0000	0.011
	2.632	1.0000	0.010
-2	2.704	0.9999	0.016
	2.693	0.9999	0.017
-3	2.657	1.0000	0.011
-4	2.764	0.9996	0.033
	2.750	0.9999	0.016
-5	2.611	0.9994	0.040
	2.651	0.9996	0.032
-6	2.768	1.0000	0.011
	2.749	0.9998	0.024

Instrument I.D.	Least Squares Slope (mm/volt)	Correlation Coefficient (r^2)	Sample Variance Sy (mm)
E11-1	2.594	0.9998	0.024
-2	2.782	0.9994	0.042
-3	2.777	0.9998	0.022
E12-1	2.696	0.9999	0.013
-2	2.719	0.9999	0.015
-3	2.742	0.9995	0.040
-4	2.763	0.9985	0.067
-5	2.786	0.9986	0.063
-6	2.894	0.9990	0.054
E13-1	2.621	1.0000	0.011
-2	2.765	0.9997	0.029
-3	2.651	0.9999	0.016
-4	2.694	0.9999	0.020
-5	2.587	0.9999	0.016
-6	2.783	0.9997	0.031

APPENDIX D

CONVERGENCE POINT DATA

Tables D

Convergence Point Readings (mm)

Reading Between Anchors No.	Top Heading 2+68	2+76	2+83	2+89	2+96	3+02	3+11	3+19	3+27	3+35	3+42	3+49	3+57
CA1 - CA2	0	0.05	0 (rezero)	-0.28 -0.21	-0.13 -0.30	-0.38 -0.23	-0.43 -0.36	-0.51 -0.34		-0.24	-0.66 -0.40 -0.10 -0.26		
CA3 - CA4	0 0.17		-0.20	0 (rezero) 1.13	1.10 0.86	2.17 1.39	0.94 0.93	1.13		0.98	0.94 0.93 1.02 0.89		
CA5 - CA6	0 0.01	-0.04	0.03	0 (rezero) 0.16	0.06 0.02	-0.01 -0.24	0.25 0.11 -0.17	0.11 0.04		0.06		0.02 0.10 0.06 0.00	
CA7 - CA8			0	0.27 0.62	0.16	-0.16	0.06 0.02	0.17 0.19		0.04		0.16 0.20 0.16 0.25	
CA9 - CA10			0	-0.89 -0.73	-0.85	-0.96	-0.96 -0.77 -0.85 -0.76	-0.87		-0.98		-0.70 -0.86 -0.97 -0.89	
CA11 - CA12			0	0.16 0.22	0.14	-0.07	-0.02 0.13	0.20 0.25		0.27		0.23 0.27 0.38	

Convergence Point Readings (mm)

Reading Between Anchors No.	3+62	3+70	3+77	3+86	3+95 1st	3+95 2nd	Bench 2+05	2+33	2+59	2+72	3+00	3+24*	3+60	3+94
CA1 - CA2		-0.19		-0.19 -0.04	-0.15	-0.31	-0.13	-0.34 -0.30	-0.08	-0.44 -0.13	-0.18 -0.37	-1.43 -1.73	-1.68	
CA3 - CA4		0.93		0.88 0.78	0.76	0.64	0.59	0.76 0.78	0.65		-0.61	-1.23	-1.08	
CA5 - CA6		0.17			-0.03 0.00 -0.01	-0.03	0.02	0.06 0.00	0.17	0.92 0.14	0.08 -0.26	-1.18 -1.46	-1.47	
CA7 - CA8				0.15	0.06	0.02	0.27	0.14	0.16	0.07 0.22	0.32 0.06	-1.11 -1.18	-1.29	
CA9 - CA10		-0.85		-0.99 -1.01	-0.94	-1.03	-1.26	-0.96 -1.10	-1.07	-1.33	-1.46 -1.56	-2.49	-2.79	
CA11 - CA12		0.23		0.26 0.23	0.20	0.19	0.19	0.20 0.35	0.46	0.20 0.30	0.24 0.17	-0.88 -1.26	-1.13	

* Possible damage to extensometer

Convergence Point Readings (mm)

Reading Between Anchors No.	Top Heading 3+77	(2nd) 3+95	Bench 2+05	2+33	2+59	2+72	3+00	3+24	3+60
CA29 - CA30 (2+55)	----	----	0	0.07 -0.10			0*	-1.27	-0.88
CA17 - CA18 (2+83)	0 0.11	0.07	0.07	0.09		-0.13		0*	0.08
CA33 - CA34 (3+15)			0	0.01 -0.16	1.12	0.83		0* -0.13	-0.10
CA21 - CA22 (3+45)			0	0.05 0.08			0* -0.42	0.71 0.59	1.65
CA37 - CA38 (3+75)			0	0.01	0.03	-1.35 -1.35°	-1.39 -1.38	-2.97 -2.95	-3.23

* anchor replaced (new zero)

° anchor replaced (same zero)

APPENDIX E

PLOTS OF DISPLACEMENT VERSUS ADVANCE OF FACE FOR ALL EXTENSOMETERS

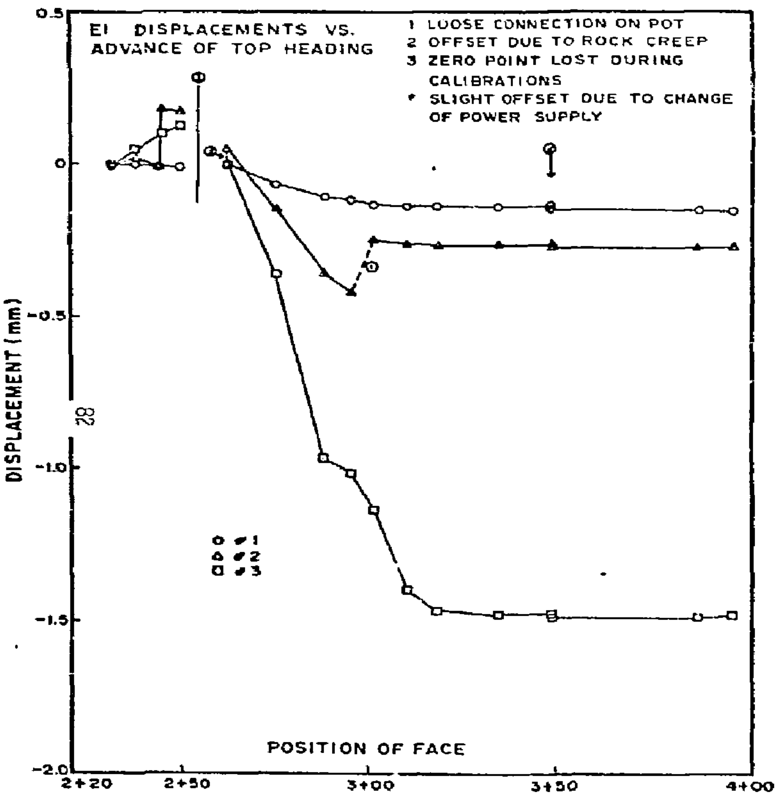

Figure E-1.

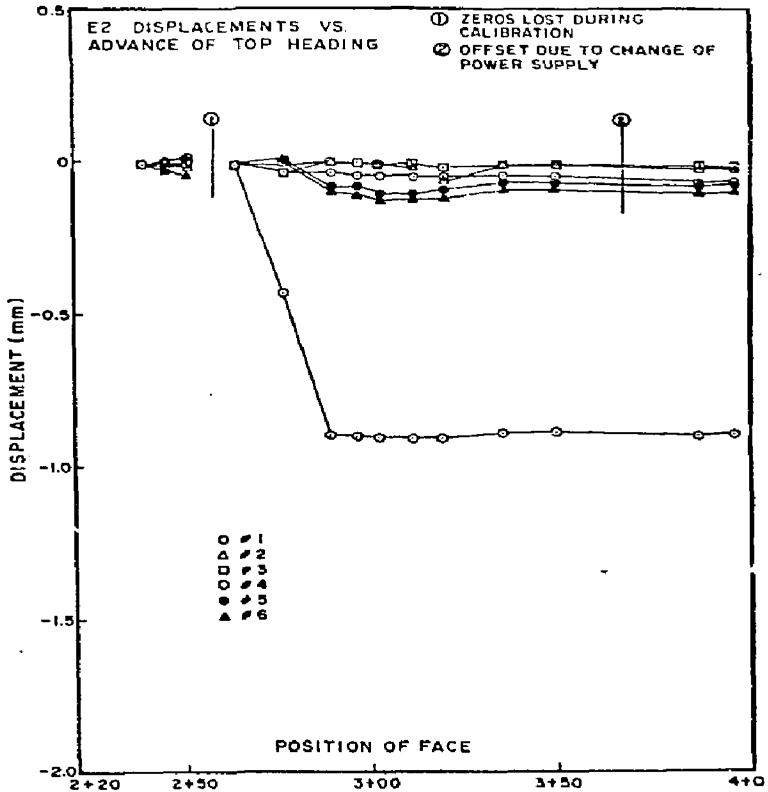

Figure E-2.

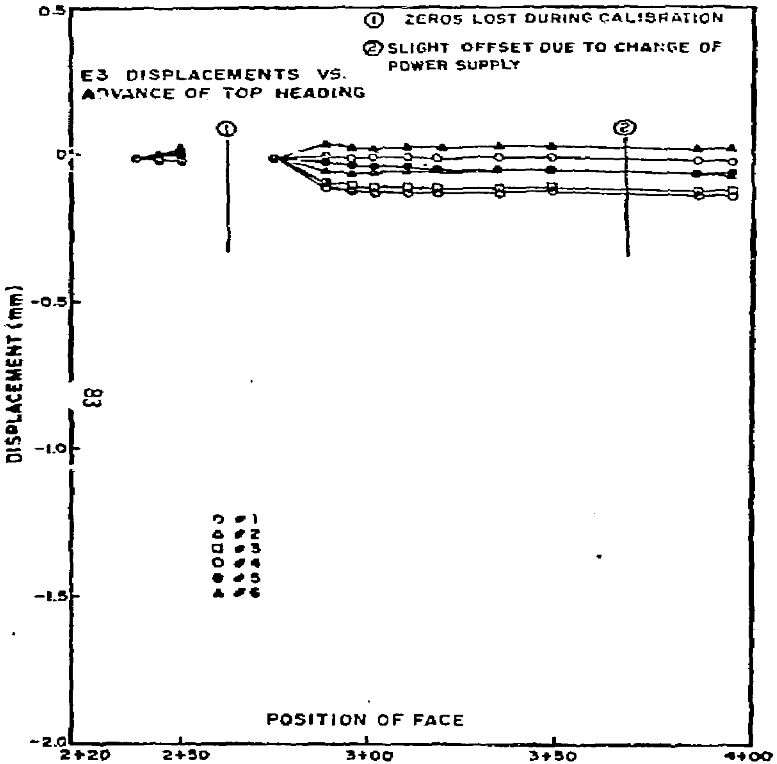

Figure E-3.

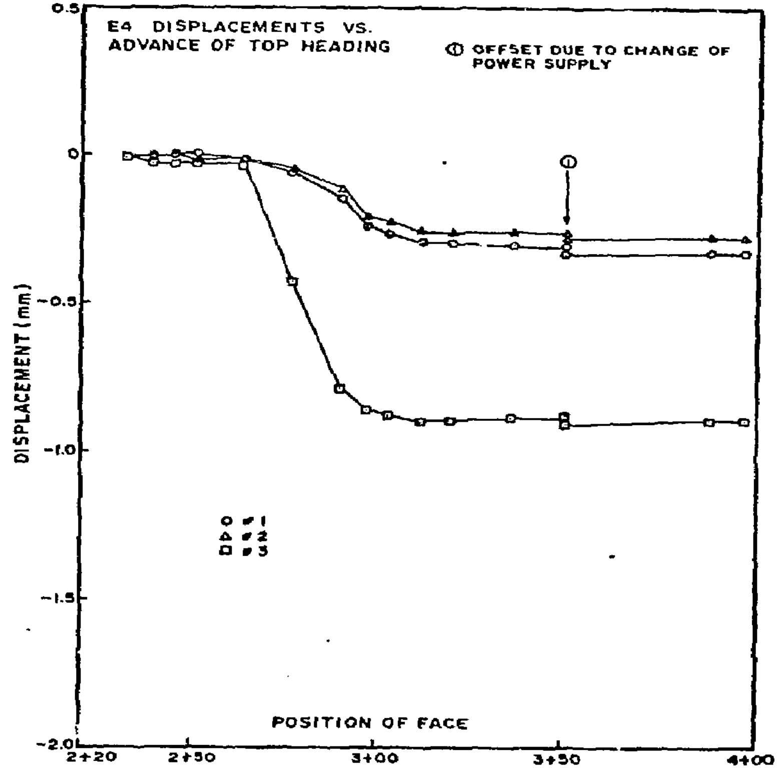

Figure E-4.

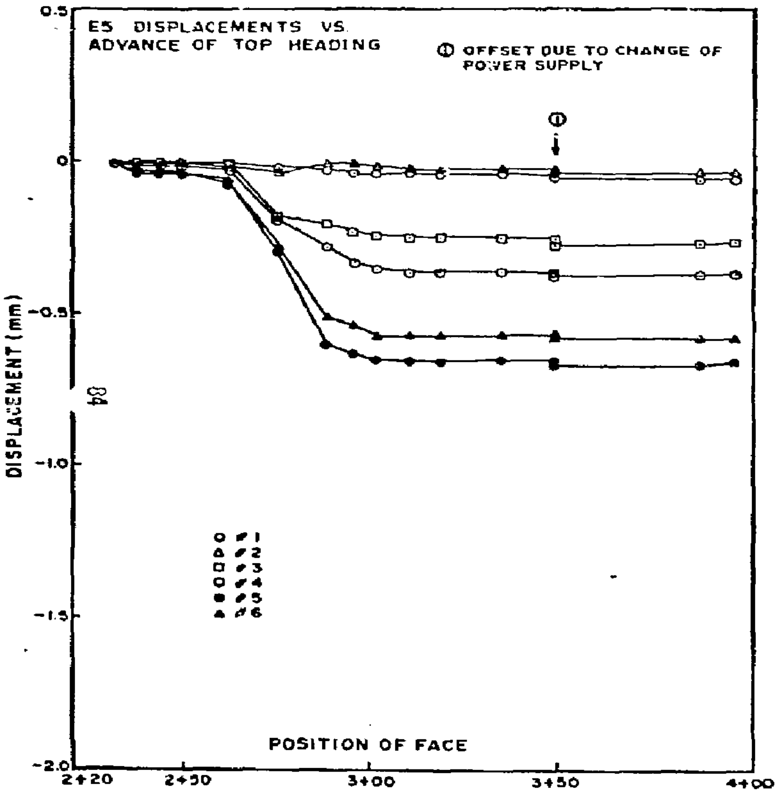

Figure E-5.

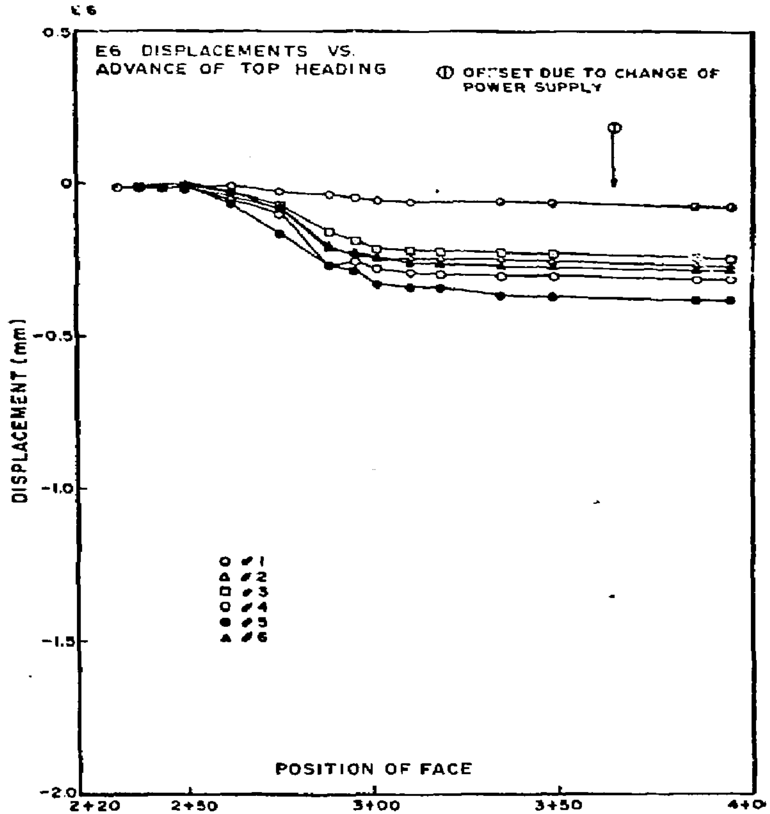

Figure E-6.

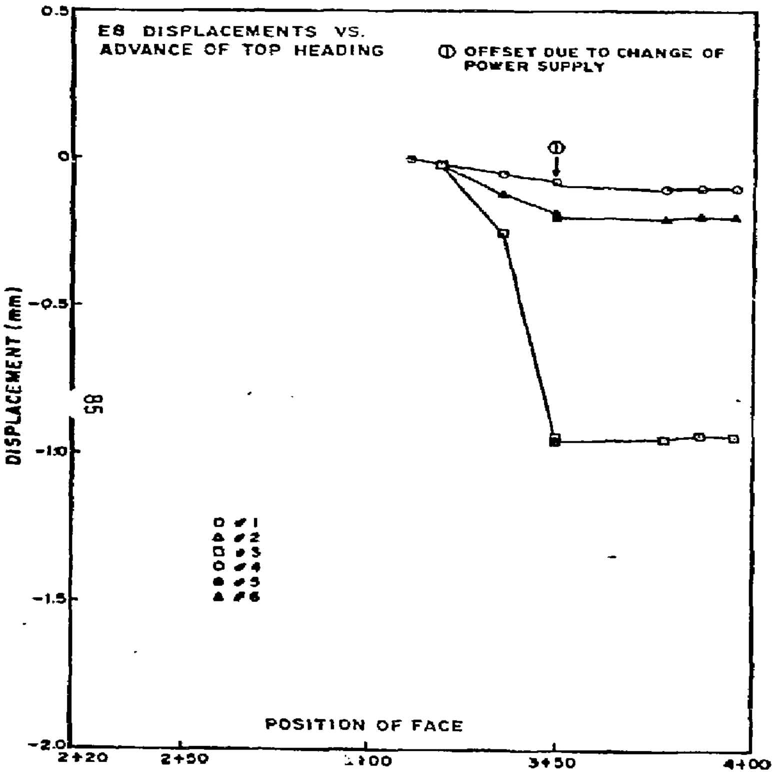

Figure E-7.

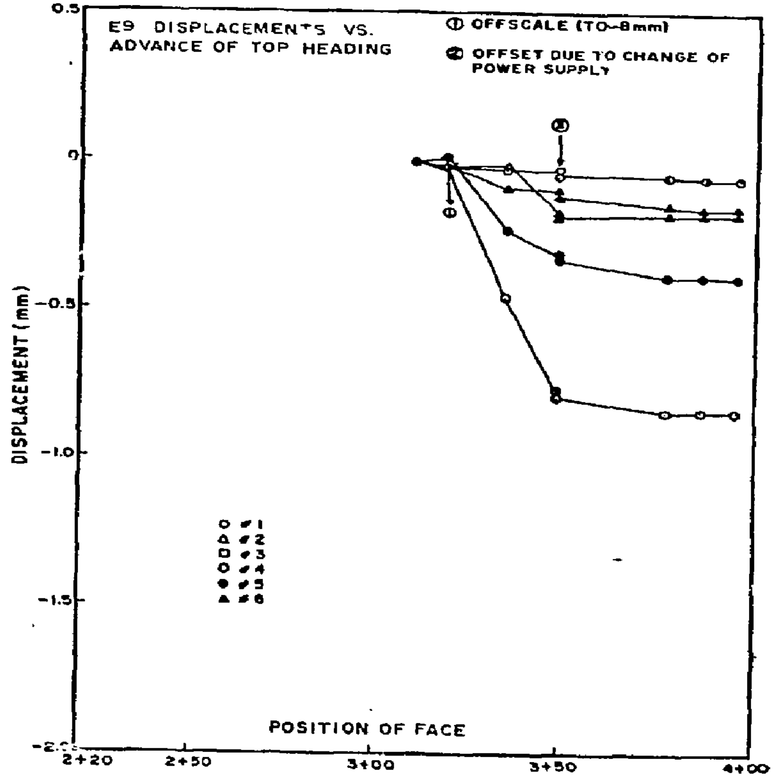

Figure E-8.

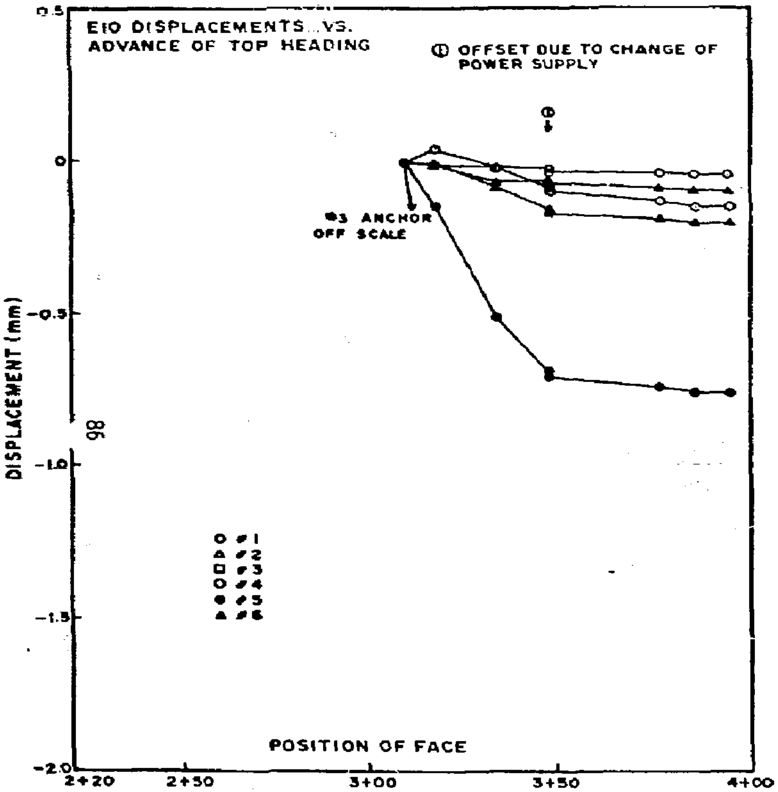

Figure E-9.

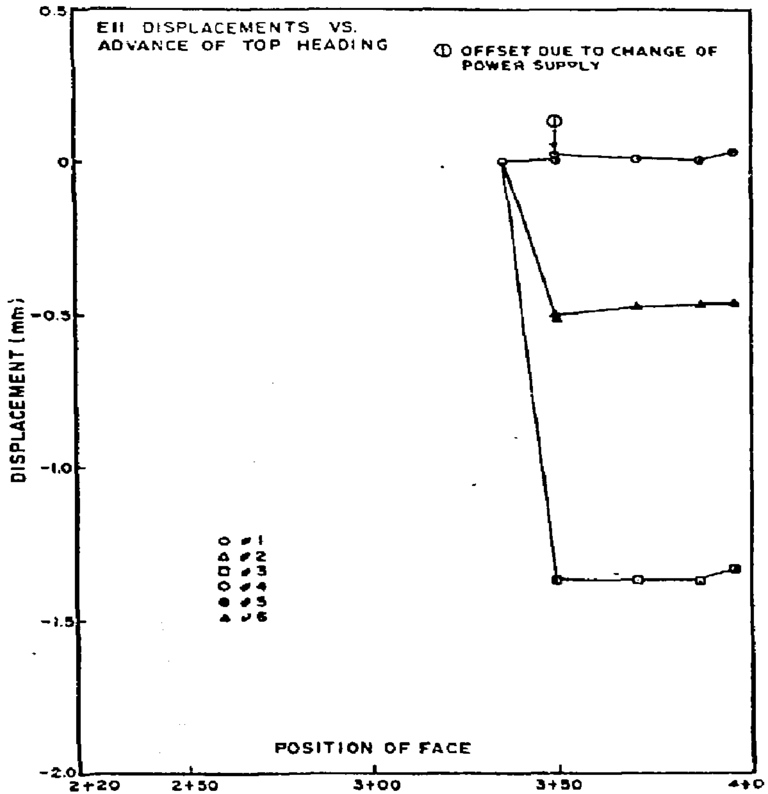

Figure E-10.

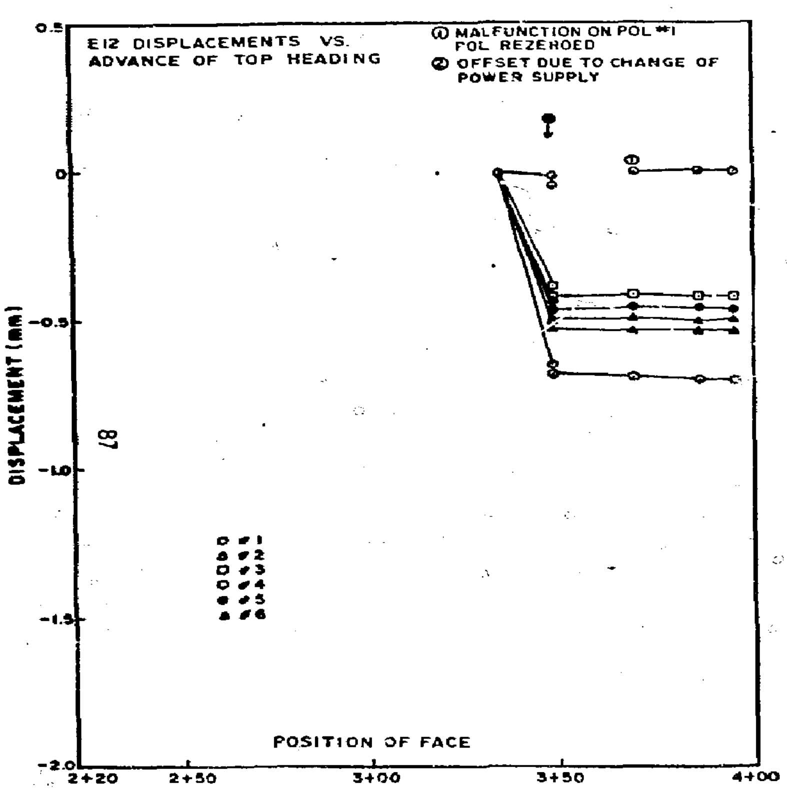

Figure E-11.

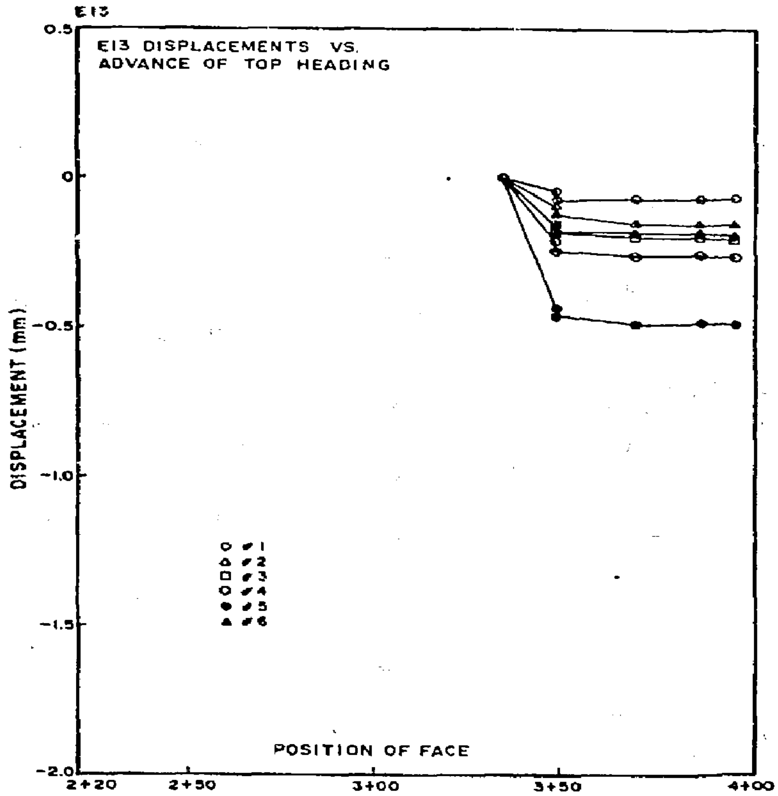

Figure E-12.

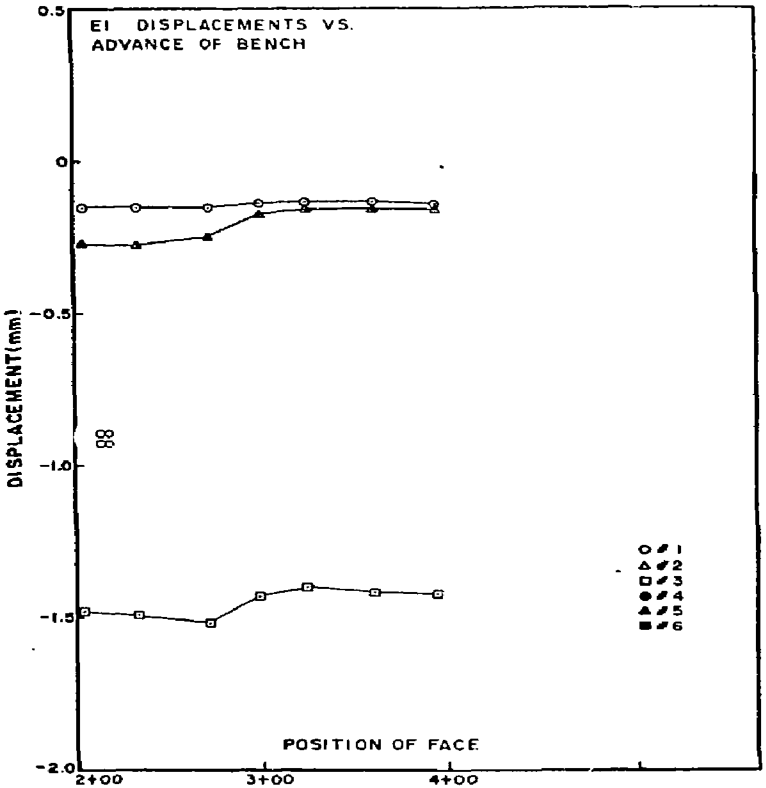

Figure E-13.

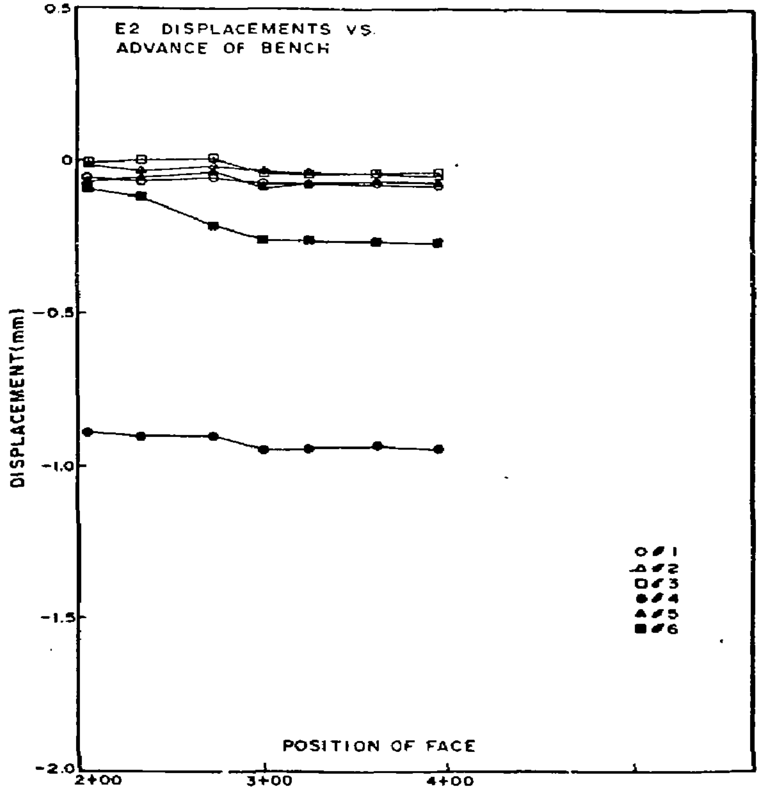

Figure E-14.

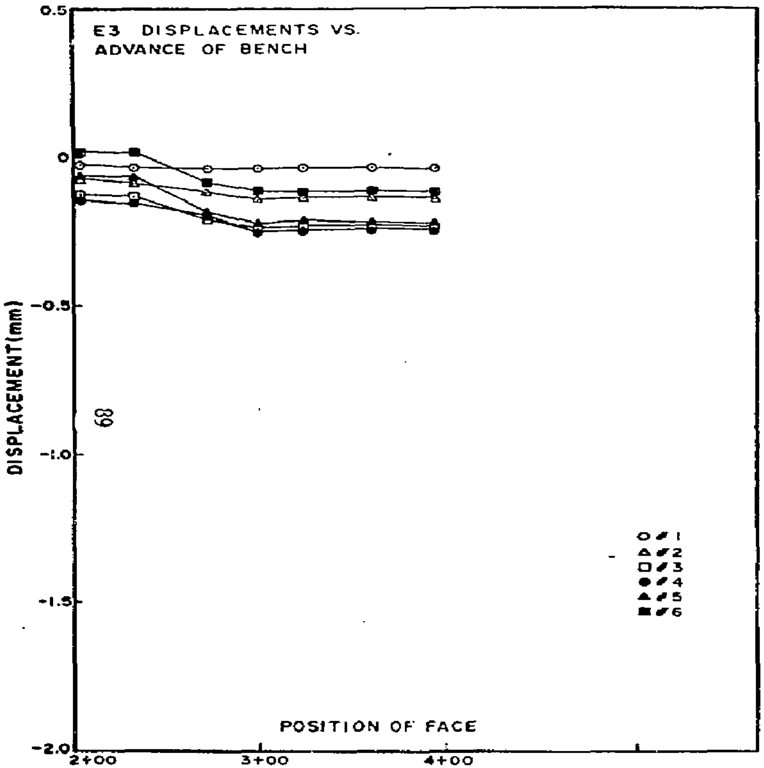

Figure E-15.

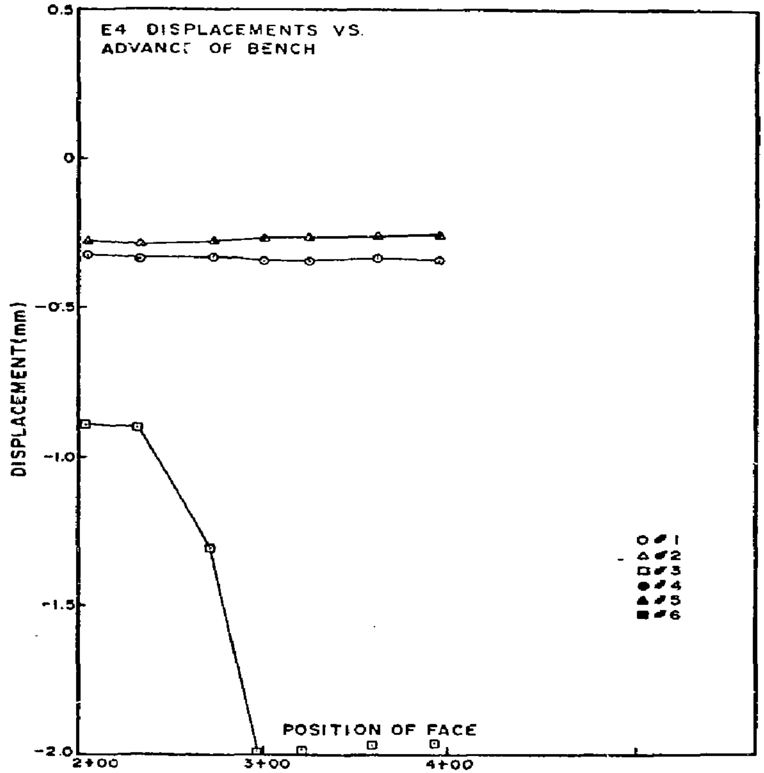

Figure E-16.

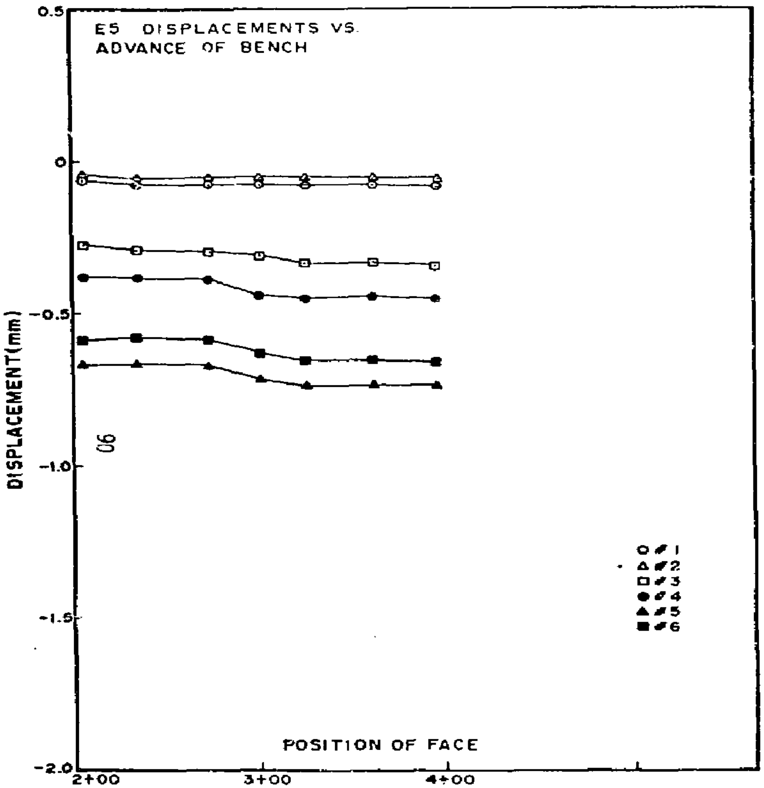

Figure E-17.

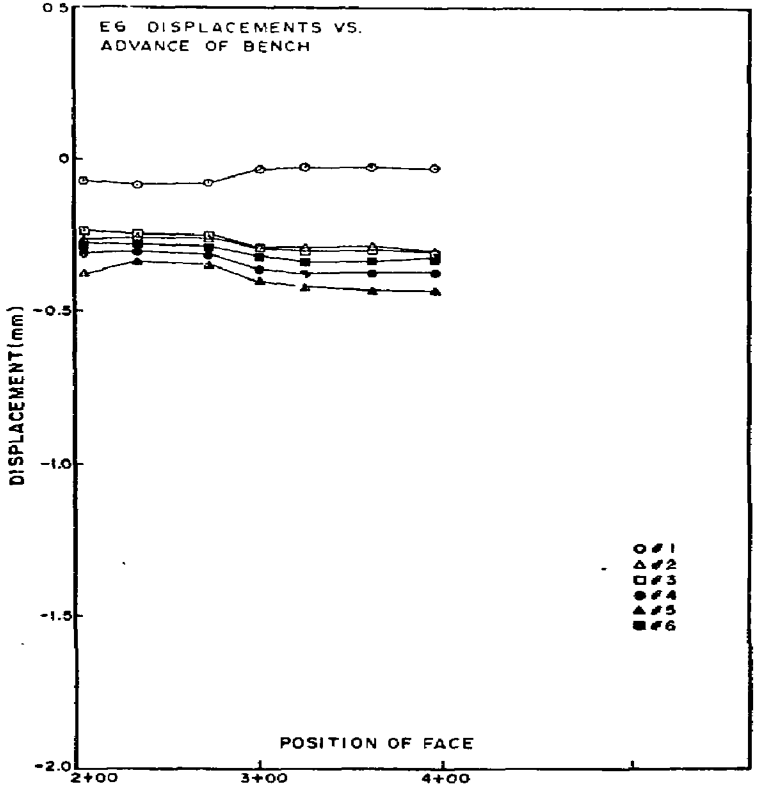

Figure E-18.

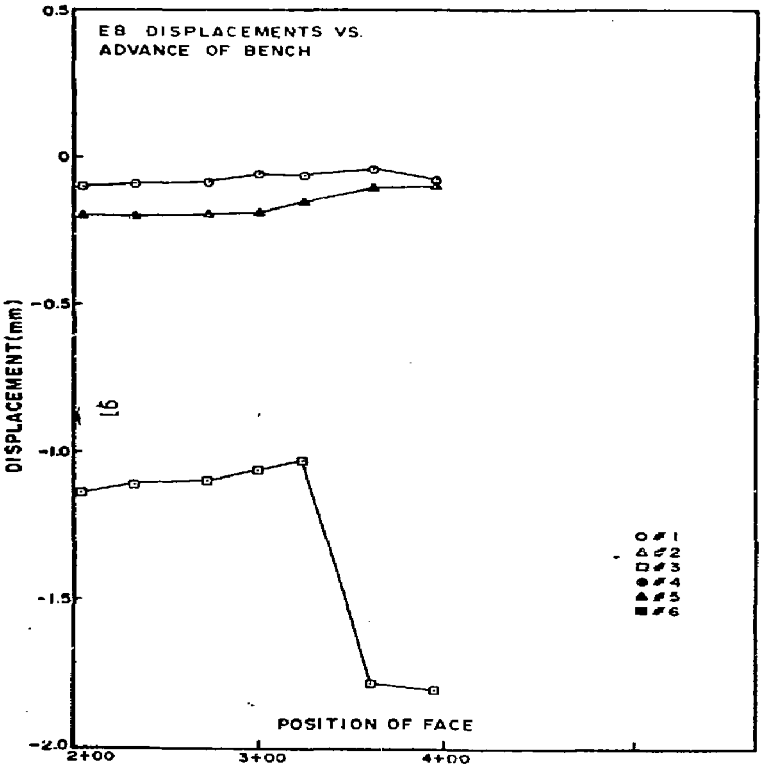

Figure E-19.

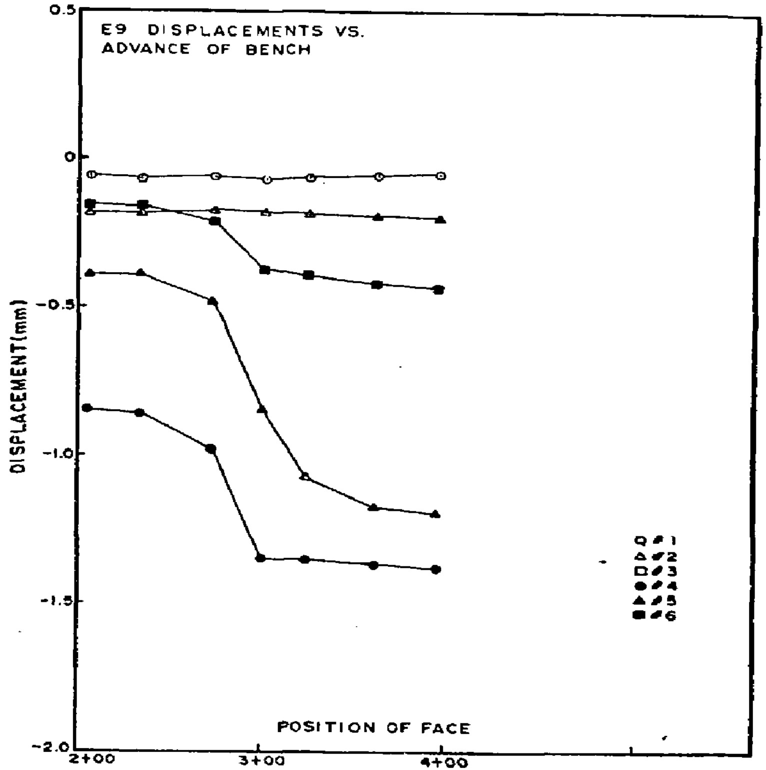

Figure E-20.

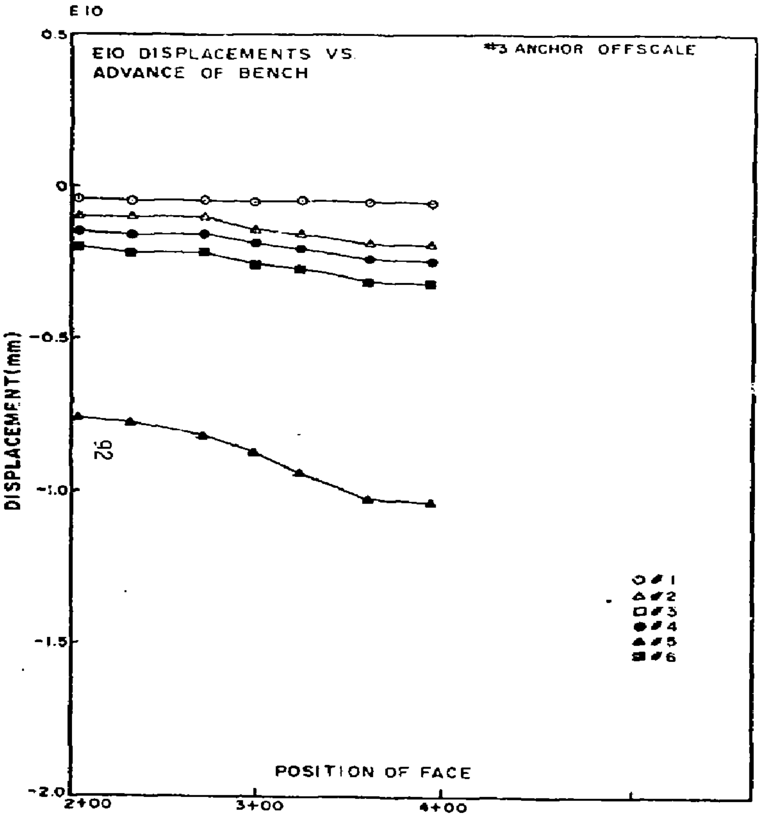

Figure E-21.

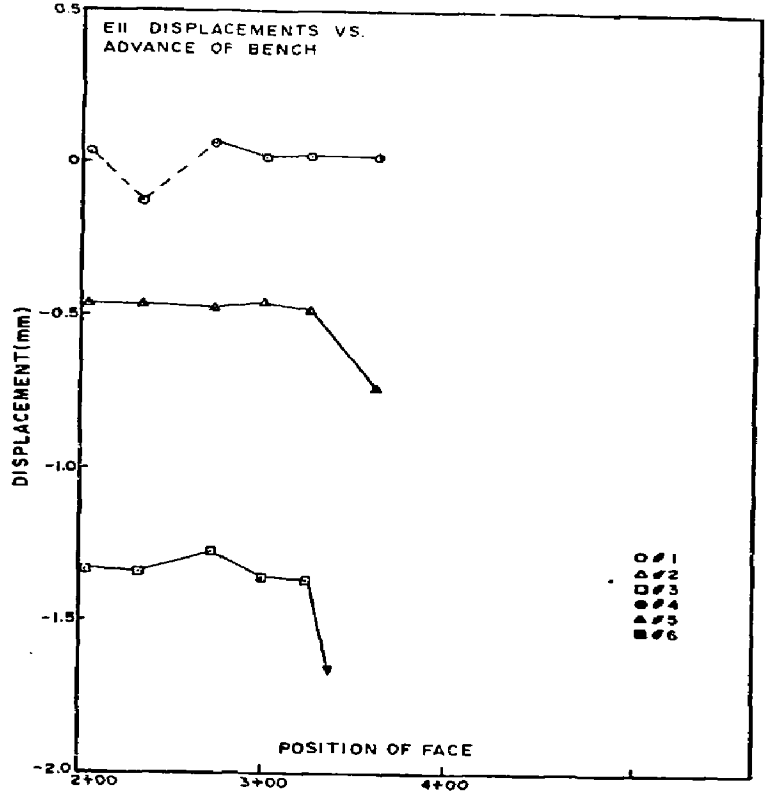

Figure E-22.

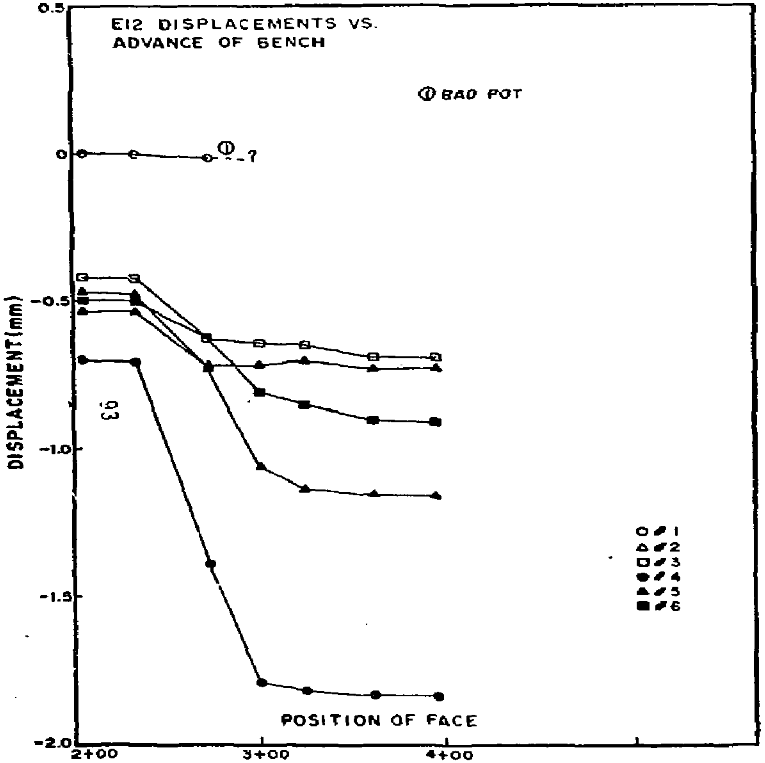

Figure E-23.

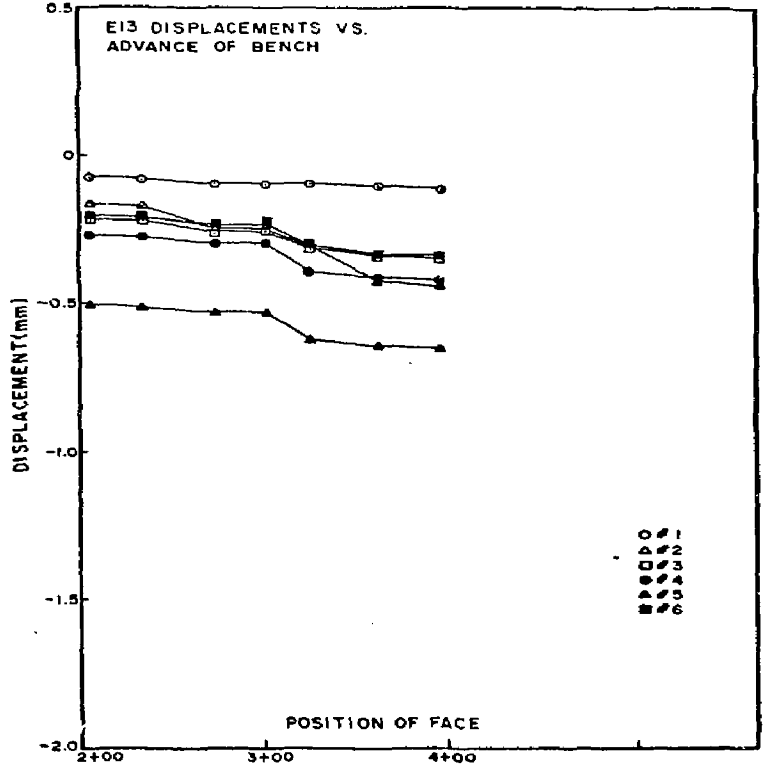

Figure E-24.

APPENDIX F

PLOTS OF CONVERGENCE VERSUS ADVANCE OF FACE

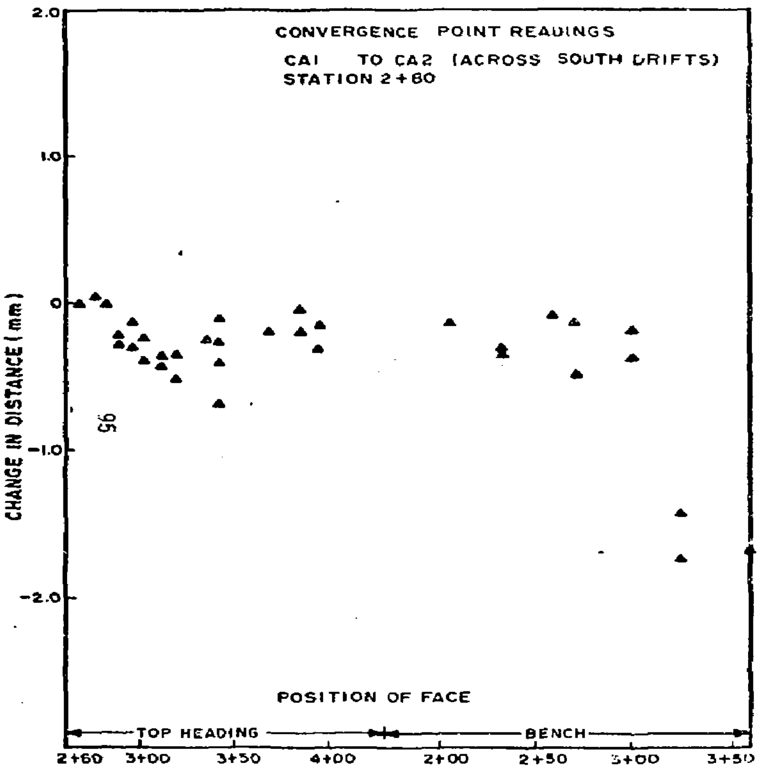

Figure F-1.

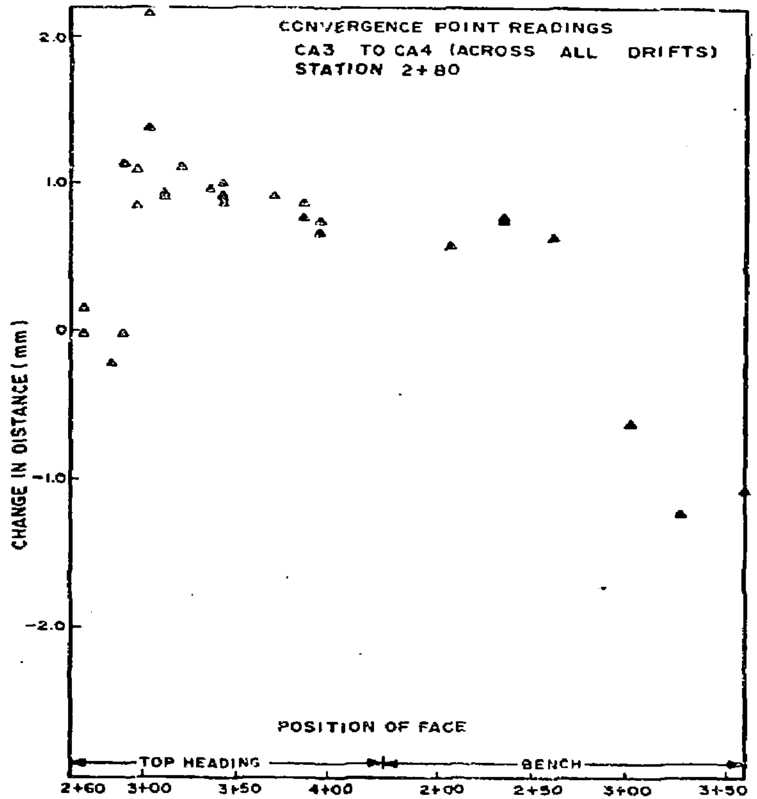

Figure F-2.

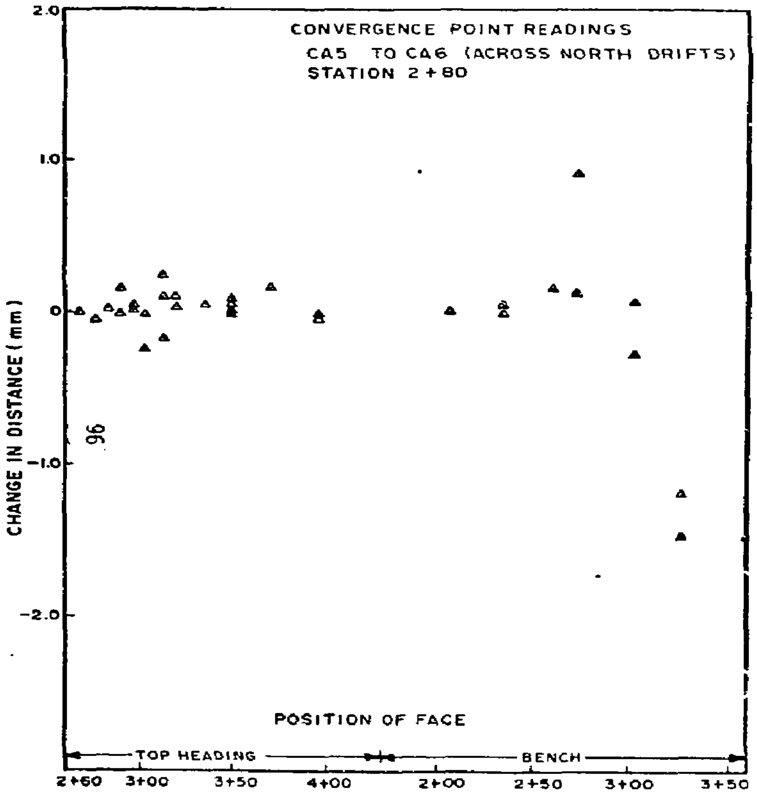

Figure F-3.

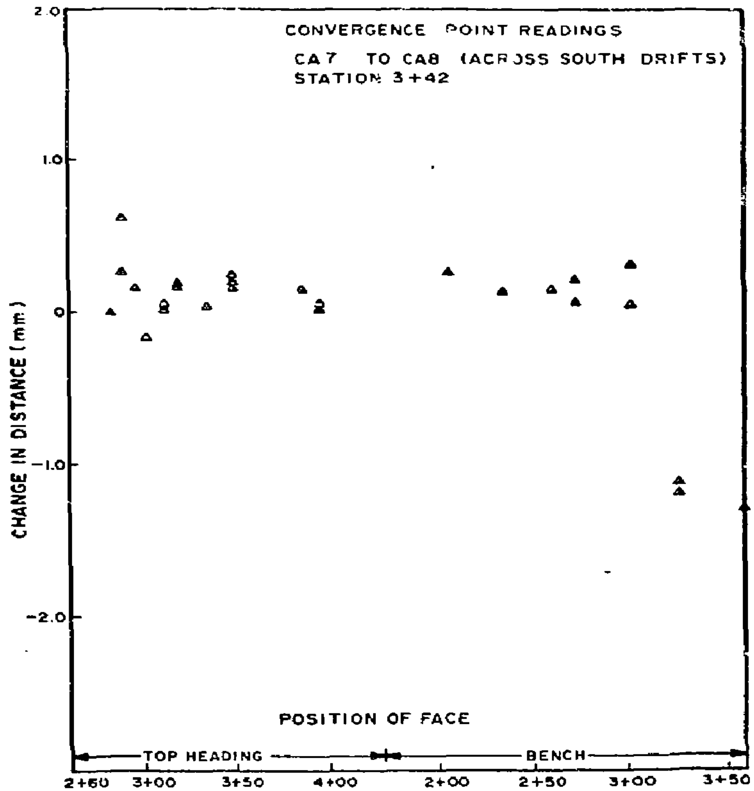

Figure F-4.

96

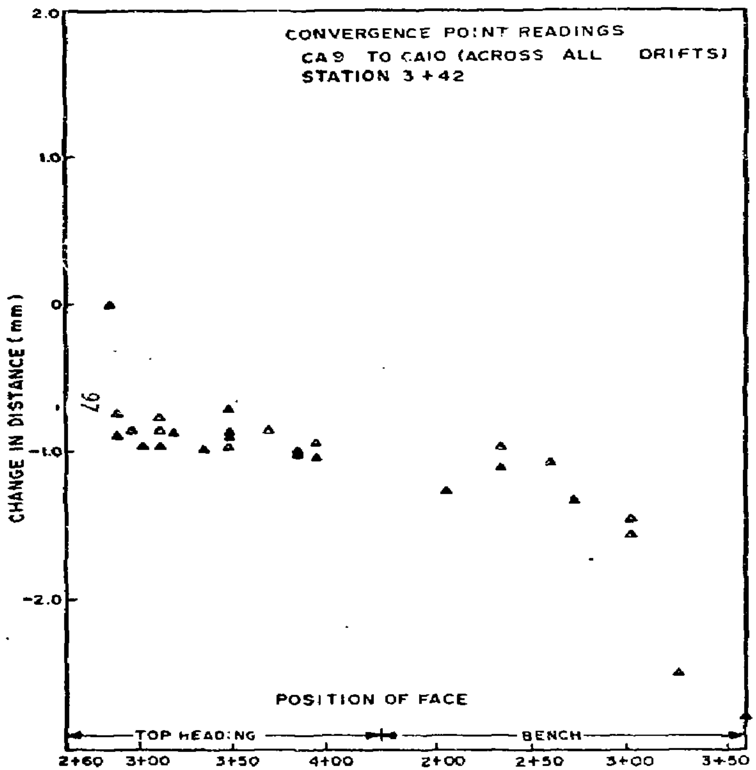

Figure F-5.

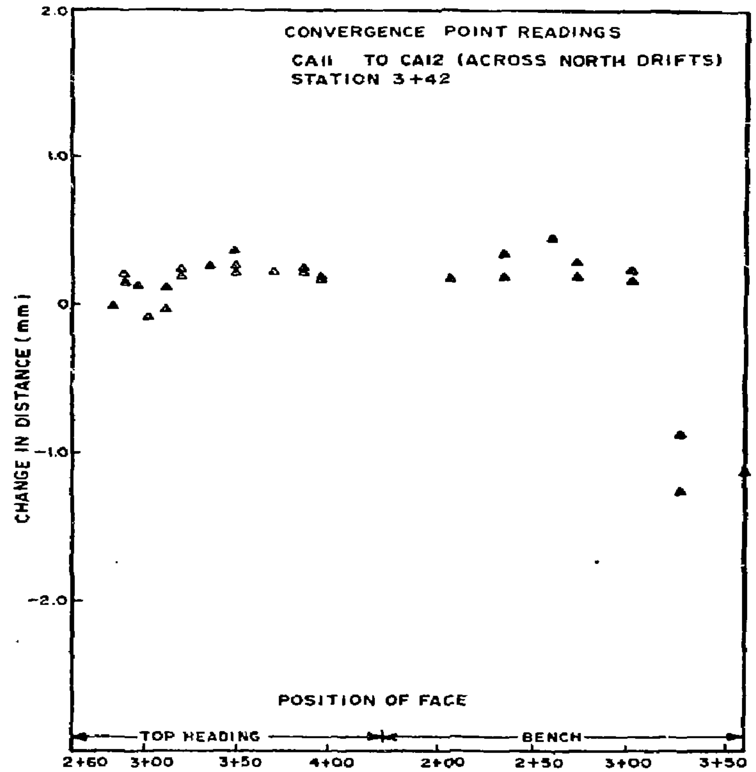

Figure F-6.

References

1. Schrauf, Todd, Personal Communication, 1979.

2. Patrick, Wes., Personal Communication, 1979.

3. St. John, C.M., Numerical and Observational Methods in Determining the Behavior of Rock Slopes in Open Cast Mines," Imperial College, Ph.D. Thesis, 1972.

4. Crouch, S.L., "Analysis of Stresses and Displacements Around Underground Excavations: An Application of the Displacement Discontinuity Method," University of Minnesota, Geomechanics Report, Nov., 1979.

5. Voegele, M.D., "Rational Design of Tunnel Supports: An Interactive Graphics Based Analysis of the Support Requirements of Excavations in Jointed Rock Masses," University of Minnesota, Ph.D. Thesis, 1978.

6. Barton, N., and Hansteen, H., "Very Large Openings at Shallow Depth: Deformation Magnitudes from Jointed Models and F.E. Analysis," Rapid Tunneling and Excavation Conference, Atlanta, Georgia, June, 1979.